

# Quark mass hierarchy and mixing via geometry of extra dimension with point interactions

Yukihiro Fujimoto,<sup>a</sup> Tomoaki Nagasawa,<sup>b</sup>  
Kenji Nishiwaki,<sup>c</sup> and Makoto Sakamoto<sup>d</sup>

<sup>a,d</sup>*Department of Physics, Kobe University, Kobe 657-8501, Japan*

<sup>b</sup>*Tomakomai National College of Technology, 443 Nishikioka, Tomakomai 059-1275, Japan*

<sup>c</sup>*Regional Centre for Accelerator-based Particle Physics, Harish-Chandra Research Institute, Allahabad 211 019, India*

## Abstract

We propose a new model which can naturally explain origins of fermion generations, quark mass hierarchy, and Cabibbo-Kobayashi-Maskawa matrix simultaneously from geometry of an extra dimension. We take the extra dimension to be an interval with point interactions, which are additional boundary points in the bulk space of the interval. Because of the Dirichlet boundary condition for fermion at the positions of point interactions, profiles of chiral fermion zero modes are split and localized, and then we can realize three generations from each five-dimensional Dirac fermion. Our model allows fermion flavor mixing but the form of non-diagonal elements of fermion mass matrices is found to be severely restricted due to geometry of the extra dimension. The Robin boundary condition for a scalar leads to an extra coordinate-dependent vacuum expectation value, which can naturally explain the fermion mass hierarchy.

---

<sup>a</sup> E-mail: 093s121s@stu.kobe-u.ac.jp

<sup>b</sup> E-mail: nagasawa@gt.tomakomai-ct.ac.jp

<sup>c</sup> E-mail: nishiwaki@hri.res.in

<sup>d</sup> E-mail: dragon@kobe-u.ac.jp

# 1 Introduction

Recently the ATLAS and CMS experimental groups of the CERN Large Hadron Collider (LHC) have announced the excess at 125 GeV, which is consistent with the Standard Model (SM) Higgs boson, with a local significance of  $5\sigma$  after combining 7 TeV and 8 TeV data [1, 2]. This amazing thing means mysteries behind the last missing piece of the SM are ready to be unveiled. But the SM still has many points which are unclear in spite of lots of effort of physicists.

One is called “quark mass hierarchy problem”. In the SM, we are forced to comply with hierarchy of almost five orders of magnitude in Yukawa couplings of quarks for describing the suitable quark masses. Closely related to this issue, the SM cannot answer the mechanism behind the Cabibbo-Kobayashi-Maskawa (CKM) matrix, which describes the strengths of generation-changing interactions in the SM. In addition to the two issues, we cannot explain why we introduce three copies of quarks whose quantum numbers are the same except their masses and the degrees of mixings in the above interactions. Many attempts have been done for explaining the issues within four dimensional (4D) Quantum Field Theory (QFT) framework with, *e.g.*, launching new continuous and/or discrete symmetry, introducing new matters and interactions, discussing renormalization group (RG) effects from a theory in a (very) high energy scale compared to the EW (ElectroWeak) scale.

When we focus on the case in five dimension (5D), where there is one additional spatial direction, we can find a new useful tool for tackling the above and the other problems, *geometry*. Two of the most renowned studies which show the power of geometry are [3, 4], where the authors proposed innovative ways for solving hierarchy problem. Extra space can have a huge variety of structure, which are detected as differences in 4D effective theory point of view. In 5D QFT framework, we also find new mechanisms which we cannot find in 4D, *e.g.*, generating spontaneous gauge symmetry breaking by global Wilson loop operator [5–7], symmetry breaking by orbifold boundary conditions (BCs) [8–10]. It, however, seems to be hard to answer the origins of the quark mass hierarchy, the quark mixing and the number of fermion generation only based on them. We comment that the existence of (compact) extra dimension(s) is suggested by the superstring theory. Lots of works have been done for settling the three problems in the quark (and lepton sectors) independently and/or simultaneously in the many contexts of large extra dimension [11–14], warped extra dimension [15–17], vortex profile [18–20] based on [21], and others [22–24].

In this paper, we focus on one of the interesting mechanisms due to extra dimension, *i.e.*, localization of fields. We can generate the hierarchy in the Yukawa coupling naturally when the SM fermions are localized at different points in one (more) extra dimension(s) [25], whose situation is realized by a 5D scalar field coupling to 5D fermions with a kink background [26, 27]. A variation of this possibility is to localize the Higgs scalar vacuum expectation value (VEV) in one extra dimension [28, 29]. Here we propose a simple way of realizing three chiral generations and their localization, where we introduce point interactions (or many branes) on an interval [30–33]. This system is decomposed into multi intervals and due to the Dirichlet BC at the positions of point interactions, and fermion zero modes are split and degenerated. Each profile is localized around a corresponding point interaction as an effect of nonzero fermion bulk mass.

When we construct a model with the above mechanism, it is reasonable to assume all the 5D fields live in the bulk with no tree-level localized term at the positions of point interactions. This setup is very similar to the minimal Universal Extra Dimension (mUED) model on  $S^1/Z_2$  [34]. The mUED is one of the most investigated models in context of extra dimension and has many gripping points, *e.g.*, existence of dark matter candidate is ensured by the accidental symmetry

under changing the two end points of  $S^1/Z_2$  [35].<sup>1</sup> The latest concrete analysis for relic abundance of the candidate is found in Ref. [40]. The parameters of the mUED (and other six dimensional UED models) are restricted by the analyses based on recent LHC experimental results in Refs [41–45]. In the mUED model, the Yukawa structure is the same with that of the SM, and therefore we still need the fine tuning in the coefficients. On the other hand, in our model, the 5D Yukawa couplings cannot possess generation index since one generation of the SM fields is introduced. In other words, another maneuver should be offered to overwhelm the difficulty.

To generate the Yukawa coupling hierarchy via geometry, an extra coordinate-dependent and localized profile of the scalar VEV is preferred. An idea to realize this situation is to impose nontrivial BCs for the scalar field which is incompatible with its non-vanishing constant vacuum configuration. This mechanism has been applied to breaking translational invariance [46], breaking supersymmetry [47–50] and extended to higher extra dimensions [51, 52]. For the scalar singlet case, the profile is described with the Jacobi’s elliptic function and we can find a parameter region where the elliptic function approaches the exponential function. The exponential form is ideal for generating large hierarchy within a natural choice of parameters and almost all the input parameters take coefficients with  $\mathcal{O}(10)$  magnitude when we scale them based on each corresponding suitable mass value.

This paper is organized as follows: In Section 2 we give a brief review on a way of constructing system with many point interactions briefly and subsequently, debate about suitable choices of BCs for 5D fermion and vector fields. In Section 3 we search for the possibility for achieving quark mass hierarchy and mixing simultaneously in multi point interaction system with an exponential Higgs VEV profile. In Section 4 we construct a concrete model realizing the exponential VEV with high precision without violating gauge coupling universality and check the validity of the model through discussing naturalness of magnitudes of coefficients. Section 5 is devoted to conclusions and discussions.

## 2 Basic properties of zero mode functions in system with point interactions

### 2.1 Zero mode profile of 5D fermion on an interval with a point interaction

In this subsection, we consider the zero mode profile of 5D fermion on an interval with a point interaction, where is put in the middle of the whole system. A point interaction means that the interaction can occur only at a point as a  $\delta$ -function potential. In Refs. [53–56], possible point interactions in one-dimensional quantum mechanics are shown to be classified by boundary conditions which are characterized by  $U(2)$  parameters for a circle and  $U(1) \times U(1)$  for an interval. According to this result, we will specify each point interaction by one of the possible boundary conditions in this paper. We use a coordinate  $y$  to indicate the position in the extra space and assign the locations of the three boundary points as  $0 (= L_0), L_1, L_2$ , respectively. The schematic diagram of our system in Fig. 1 helps our understanding.

In this paper, we concentrate on a simple case, where there is no tree-level brane localized term.

---

<sup>1</sup> Recently a non-minimal version of UED model with brane-localized terms has been proposed in Ref. [36] and the collider physical studies on the model have been also done in Refs. [36–39].

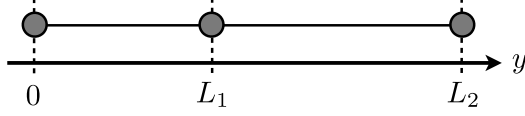


Figure 1: A schematic diagram of the interval system with a point interaction at  $y = L_1$ .

The 5D action of a fermion we consider is

$$\int d^4x \left[ \int_0^{L_1} dy + \int_{L_1}^{L_2} dy \right] \left( \bar{\Psi} (i\partial_M \Gamma^M + M_F) \Psi \right), \quad (1)$$

where the latin indices run 0 to 3, 5 (or  $y$ ) and greek ones run 0 to 3, respectively.<sup>2</sup>  $\Psi$  and  $M_F$  are a 5D Dirac fermion and its bulk mass. We mention that 5D fermion bulk mass with the ordinary form is allowed in our system since we do not introduce orbifold  $Z_2$  parity.

In what follows, we contemplate profiles of fermions. Due to variational principle, the following quantities must vanish at the corresponding boundaries as

$$\left[ \bar{\Psi} \Gamma^y \delta \Psi \right] \Big|_{y=0} = \left[ \bar{\Psi} \Gamma^y \delta \Psi \right] \Big|_{y=L_2} = 0, \quad (2)$$

$$\left[ \bar{\Psi} \Gamma^y \delta \Psi \right] \Big|_{y=L_1-\varepsilon} - \left[ \bar{\Psi} \Gamma^y \delta \Psi \right] \Big|_{y=L_1+\varepsilon} = 0, \quad (3)$$

where  $\varepsilon$  is an infinitesimal positive constant. The form of  $\bar{\Psi} \Gamma^y \delta \Psi = 0$  can be decomposed into  $\bar{\Psi}_R \delta \Psi_L = \bar{\Psi}_L \delta \Psi_R = 0$ , where the 4D chirality is defined as  $\gamma^5 \Psi_L = \pm \Psi_L$ . Then, the Dirichlet BCs turn out to be consistent with Eqs. (2) and (3), *i.e.*

$$\Psi_R = 0 \quad \text{or} \quad \Psi_L = 0 \quad \text{at} \quad y = 0, L_1 \pm \varepsilon, L_2. \quad (4)$$

We will, however, choose  $\Psi_R = 0$  at all the boundaries (or  $\Psi_L = 0$  at them) to realize the SM chiral fermions in the zero mode sector, as we will see later.

We mention that once the BC of a right- (left-) handed part of a 5D fermion  $\Psi$  is determined as

$$\Psi_R(x, L_i) = 0 \quad \left( \Psi_L(x, L_i) = 0 \right), \quad (5)$$

where  $L_i$  shows the position of a boundary point, the BC of the remaining left- (right-) handed part is simultaneously fixed through equation of motion (EOM) as

$$(-\partial_y + M_F) \Psi_L = 0 \quad \left( (\partial_y + M_F) \Psi_R = 0 \right) \quad \text{at} \quad y = 0, L_1 \pm \varepsilon, L_2. \quad (6)$$

We can expand the 5D fermion as

$$\begin{aligned} \Psi(x, y) &= \Psi_R(x, y) + \Psi_L(x, y) \\ &= \sum_n \left\{ \psi_R^{(n)}(x) f_{\Psi_R^{(n)}}(y) + \psi_L^{(n)}(x) f_{\Psi_L^{(n)}}(y) \right\}. \end{aligned} \quad (7)$$

<sup>2</sup> In this paper, we choose metric convention as  $\eta_{MN} = \eta^{MN} = \text{diag}(-1, 1, 1, 1, 1)$ . The representations of gamma matrices are  $\Gamma_\mu = \gamma_\mu$ ,  $\Gamma_y = \Gamma^y = -i\gamma^5 = \gamma^0\gamma^1\gamma^2\gamma^3$  and we pay attention to the Clifford algebra is defined as  $\{\Gamma_M, \Gamma_N\} = -2\eta_{MN}$ .

The series of  $\{f_{\Psi_R^{(n)}}\}$  and  $\{f_{\Psi_L^{(n)}}\}$  are eigenstates of the hermitian operators  $\mathcal{D}^\dagger \mathcal{D}$  and  $\mathcal{D} \mathcal{D}^\dagger$ , respectively; the  $\mathcal{D}$  (and  $\mathcal{D}^\dagger$ ) are defined as

$$\begin{cases} \mathcal{D} := \partial_y + M_F \\ \mathcal{D}^\dagger := -\partial_y + M_F \end{cases} , \quad (8)$$

$$\begin{cases} \mathcal{D}^\dagger \mathcal{D} f_{\Psi_R^{(n)}}(y) = M_{\Psi^{(n)}}^2 f_{\Psi_R^{(n)}}(y) \\ \mathcal{D} \mathcal{D}^\dagger f_{\Psi_L^{(n)}}(y) = M_{\Psi^{(n)}}^2 f_{\Psi_L^{(n)}}(y) \end{cases} , \quad (9)$$

where  $M_{\Psi^{(n)}}$  is a KK mass of the  $n$ -th right/left KK mode. This mass degeneracy is ensured by quantum mechanical supersymmetry (QMSUSY) [56–59] as

$$\begin{cases} \mathcal{D} f_{\Psi_R^{(n)}}(y) = M_{\Psi^{(n)}} f_{\Psi_L^{(n)}}(y) \\ \mathcal{D}^\dagger f_{\Psi_L^{(n)}}(y) = M_{\Psi^{(n)}} f_{\Psi_R^{(n)}}(y) \end{cases} . \quad (10)$$

For zero mode ( $M_{\Psi^{(0)}} = 0$ ), Eq. (10) takes the simple forms as

$$\begin{cases} \mathcal{D} f_{\Psi_R^{(0)}}(y) = 0 \\ \mathcal{D}^\dagger f_{\Psi_L^{(0)}}(y) = 0 \end{cases} . \quad (11)$$

Taking account of the BCs, we find the zero mode solutions for  $\Psi_L = 0$  at  $y = 0, L_1 \pm \varepsilon, L_2$  as (see Fig. 2)

$$f_{\Psi_{1R}^{(0)}}(y) = \begin{cases} \mathcal{N}_1 e^{-M_F y} & \text{for } 0 < y < L_1 \\ 0 & \text{for } L_1 < y < L_2 \end{cases} \quad (12)$$

and

$$f_{\Psi_{2R}^{(0)}}(y) = \begin{cases} 0 & \text{for } 0 < y < L_1 \\ \mathcal{N}_2 e^{-M_F y} & \text{for } L_1 < y < L_2 \end{cases} ; \quad (13)$$

for  $\Psi_R = 0$  at  $y = 0, L_1 \pm \varepsilon, L_2$  as

$$f_{\Psi_{1L}^{(0)}}(y) = \begin{cases} \mathcal{N}'_1 e^{M_F y} & \text{for } 0 < y < L_1 \\ 0 & \text{for } L_1 < y < L_2 \end{cases} \quad (14)$$

and

$$f_{\Psi_{2L}^{(0)}}(y) = \begin{cases} 0 & \text{for } 0 < y < L_1 \\ \mathcal{N}'_2 e^{M_F y} & \text{for } L_1 < y < L_2 \end{cases} , \quad (15)$$

where  $\mathcal{N}_1, \mathcal{N}_2, \mathcal{N}'_1, \mathcal{N}'_2$  are normalization constants, whose concrete forms are shown soon later.

Here we would like to comment on some important points of the situation. The Dirichlet boundary condition (5) for fermion at  $y = L_1$  turns out to effectively split the interval into two segments. Then, chiral zero modes are two-fold degenerate, and each profile of the zero modes is confined in one of the segments and localized exponentially at one of the edges,<sup>3</sup> as shown in Eqs. (12) and (13) (or (14) and (15)). Thus, we can realize a model with two generations of 4D chiral fermions in the case of the interval with a point interaction. Furthermore, the localization of the zero mode profiles will be found to lead to the fermion mass hierarchy, as will see later. We can see pictures explaining this situation in Fig. 2. Each concrete form is written down as follows:

---

<sup>3</sup> It is noted that the value of  $M_F$  can take a negative value and in this case, the direction of wave function localization flips to the opposite side.

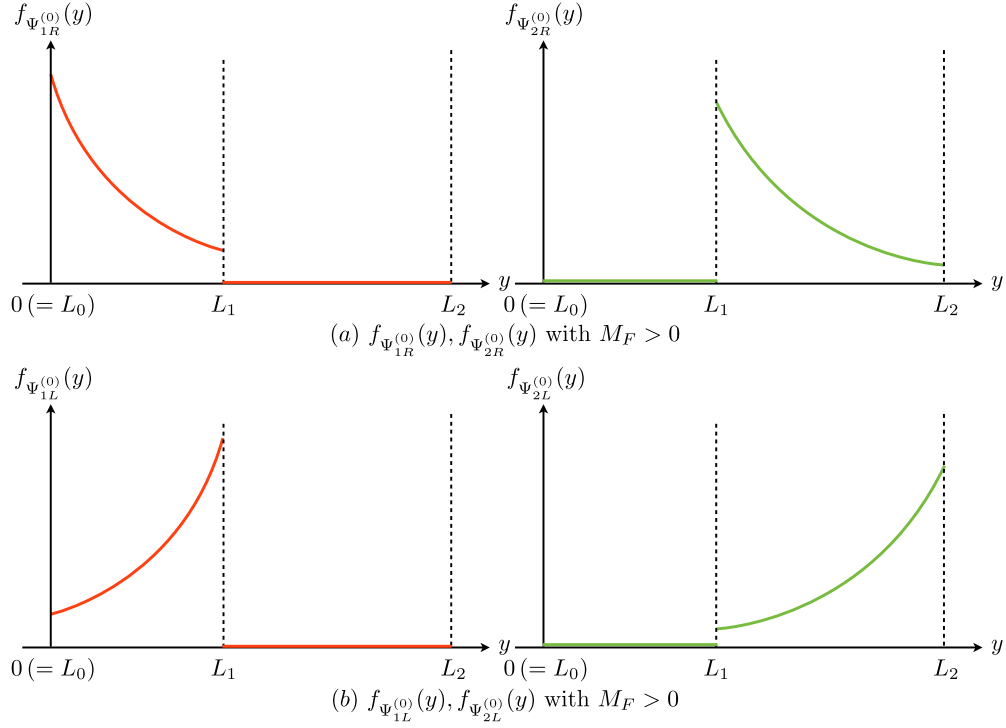


Figure 2: Profiles of the zero modes  $f_{\Psi_{1R}}^{(0)}(y)$ ,  $f_{\Psi_{2R}}^{(0)}(y)$  ( $f_{\Psi_{1L}}^{(0)}(y)$ ,  $f_{\Psi_{2L}}^{(0)}(y)$ ) are schematically depicted in (a) ((b)) for  $\Psi_L = 0$  ( $\Psi_R = 0$ ) with  $M_F > 0$ . Here there are the three boundary points at  $y = 0, L_1, L_2$ .

- In the case of  $\Psi_R = 0$  at  $y = 0, L_1 \pm \varepsilon, L_2$ ,

$$\begin{aligned} \Psi(x, y) = & \left\{ \sqrt{\frac{2M_F}{e^{2M_F\Delta L_1} - 1}} e^{M_F(y-L_0)} [\theta(y-L_0)\theta(L_1-y)] \psi_{1L}^{(0)}(x) \right. \\ & \left. + \sqrt{\frac{2M_F}{e^{2M_F\Delta L_2} - 1}} e^{M_F(y-L_1)} [\theta(y-L_1)\theta(L_2-y)] \psi_{2L}^{(0)}(x) \right\} + (\text{KK modes}), \end{aligned} \quad (16)$$

- In the case of  $\Psi_L = 0$  at  $y = 0, L_1 \pm \varepsilon, L_2$ ,

$$\begin{aligned} \Psi(x, y) = & \left\{ \sqrt{\frac{2M_F}{1 - e^{-2M_F\Delta L_1}}} e^{-M_F(y-L_0)} [\theta(y-L_0)\theta(L_1-y)] \psi_{1R}^{(0)}(x) \right. \\ & \left. + \sqrt{\frac{2M_F}{1 - e^{-2M_F\Delta L_2}}} e^{-M_F(y-L_1)} [\theta(y-L_1)\theta(L_2-y)] \psi_{2R}^{(0)}(x) \right\} + (\text{KK modes}), \end{aligned} \quad (17)$$

where  $\theta(y)$  is the step function and  $\psi_1^{(0)}$  and  $\psi_2^{(0)}$  represent two (degenerated) fermion zero modes.  $\Delta L_i$  shows the length of the corresponding  $i$ -th segment which is defined as

$$\Delta L_i = L_i - L_{i-1}. \quad (18)$$

Here every mode function is suitably normalized and we can find the factor for this purpose in front of the exponential functions.

We can also evaluate the right- or left-handed KK fermions profiles but the aim of this paper is to understand the mechanism explaining the fermion mass hierarchy. Therefore we pend this issue for a future work.

## 2.2 Zero mode profile of 5D gauge boson on an interval with a point interaction

Following the previous section, we move to the zero mode profile of 5D gauge boson on the interval with a point interaction. Here we concentrate on  $U(1)$  case since our intension is to investigate the structure of mass spectrum. The concrete form of the 5D action is

$$\int d^4x \left[ \int_0^{L_1} dy + \int_{L_1}^{L_2} dy \right] \left( -\frac{1}{4} F_{MN} F^{MN} \right), \quad (19)$$

where  $F_{MN} = \partial_M A_N - \partial_N A_M$  is the 5D field strength of the 5D  $U(1)$  gauge boson  $A_M$  and we assume that the background geometry is the same as in the fermion case. After taking variation, we focus on the forms of conditions at the boundary points as

$$\left[ (\partial_y A_\mu - \partial_\mu A_y) \delta A^\mu \right] \Big|_{y=0} = \left[ (\partial_y A_\mu - \partial_\mu A_y) \delta A^\mu \right] \Big|_{y=L_2} = 0, \quad (20)$$

$$\left[ (\partial_y A_\mu - \partial_\mu A_y) \delta A^\mu \right] \Big|_{y=L_1-\varepsilon} - \left[ (\partial_y A_\mu - \partial_\mu A_y) \delta A^\mu \right] \Big|_{y=L_1+\varepsilon} = 0. \quad (21)$$

Under the constraints, we could choose the following BCs, where the Neumann (Dirichlet) type BC is assigned for  $A_\mu$  ( $A_y$ ), like the mUED model as

$$(\partial_y A_\mu) = 0 \quad \text{at} \quad y = 0, L_1 \pm \varepsilon, L_2, \quad (22)$$

$$A_y = 0 \quad \text{at} \quad y = 0, L_1 \pm \varepsilon, L_2, \quad (23)$$

in which  $A_\mu$ 's zero mode with a constant profile is found. We mention that the compatibility between the BCs' (22) and (23) can also be shown from a viewpoint of QMSUSY [56–59]. But this configuration is problematic in a phenomenological point of view. In this setup, the zero mode profile of 4D gauge boson is also split at  $y = L_1$  and this fact means that a zero mode within an interval have limited interactions only with the particles inside the segment which the gauge boson belongs to (see Fig. 3). Since this possibility with doubly-degenerated zero modes ( $A_{1\mu}^{(0)}$  and  $A_{2\mu}^{(0)}$ ) is rejected in the SM, we have to change the BC at  $y = L_1$ . We further comment that the gauge universality in the SM is violated in this configuration and this fact gets to be another reason for discarding the system with the BCs given in (22) and (23).

To avoid the problems, the profile would like to be continuous at  $y = L_1$ . Then we put the “continuous” conditions at this point for  $A_\mu$  and  $A_y$  as

$$A_\mu \Big|_{y=L_1-\varepsilon} = A_\mu \Big|_{y=L_1+\varepsilon} \quad \text{and} \quad \partial_y A_\mu \Big|_{y=L_1-\varepsilon} = \partial_y A_\mu \Big|_{y=L_1+\varepsilon}, \quad (24)$$

$$A_y \Big|_{y=L_1-\varepsilon} = A_y \Big|_{y=L_1+\varepsilon} \quad \text{and} \quad \partial_y A_y \Big|_{y=L_1-\varepsilon} = \partial_y A_y \Big|_{y=L_1+\varepsilon}. \quad (25)$$

These conditions are consistent with the constraints in Eq. (21). In this case, we can observe only one zero mode of  $A_\mu$ , whose situation is consistent with that of the SM (see Fig. 3). It is noted that we need to put the continuity in the first derivative level because the Klein-Gordon (or Maxwell) equation is second order. We also consider this continuous condition for 5D scalar as in Eq. (25).

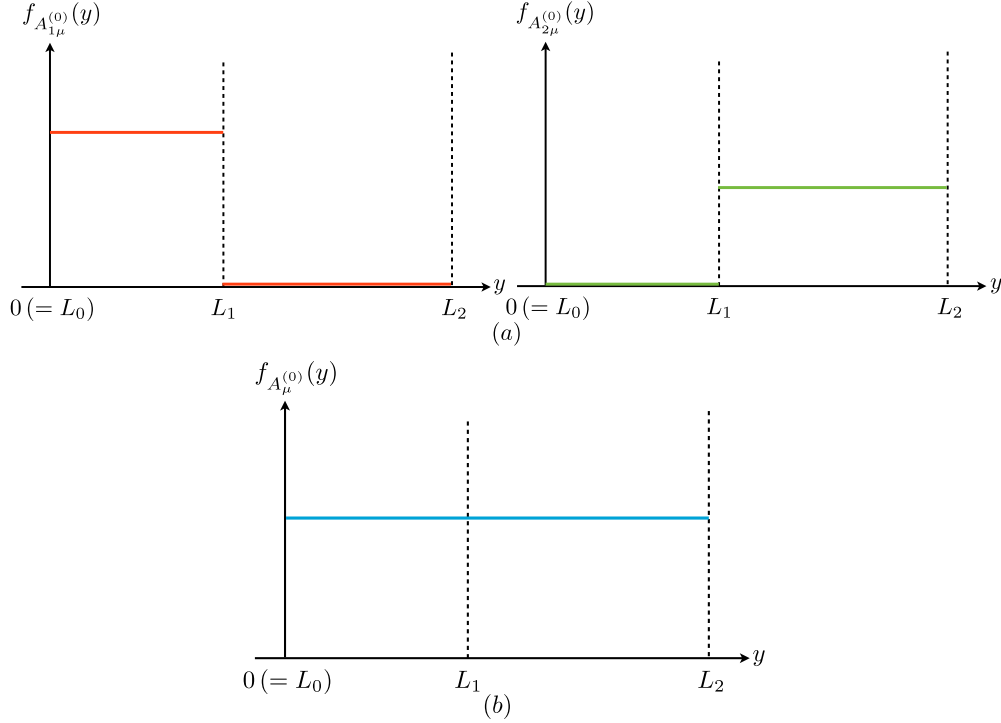


Figure 3: Profiles of zero mode 4D gauge boson with BCs in Eq. (22) in (a) and with BCs, which are modified at  $y = L_1$  as in Eq. (24) in (b).

### 2.3 Flavor mixing in system with point interactions

We can also consider the “continuous” condition at point interactions for fermions as

$$\Psi \Big|_{y=L_i-\varepsilon} = \Psi \Big|_{y=L_i+\varepsilon}, \quad (26)$$

where  $L_i$  denotes a position of point interactions. An interesting application is given as follows: At this time, we add another 5D fermion  $\Psi'$  with the different bulk mass  $M'_F$  and go to a two-point-interaction system, where the point interactions are located at  $y = L_1, L'_1$  (see Fig. 4). The 5D action which now we think about is

$$\int d^4x \int_0^{L_2} dy \left\{ \left[ \bar{\Psi} (i\partial_M \Gamma^M + M_F) \Psi \right] + \left[ \bar{\Psi}' (i\partial_M \Gamma^M + M'_F) \Psi' \right] \right\}, \quad (27)$$

where we do not divide the range of integral for  $y$  for clarity in description. The BCs for  $\Psi$  and  $\Psi'$  are selected as in Fig. 4, where the red (blue) circular spots show the Dirichlet-type BC for left- (right-) handed part at the corresponding boundary points, respectively, and the small white dots mean the continuous condition for fermions. Under the BCs, zero modes of both  $\Psi$  and  $\Psi'$  become two-fold degenerated and we distinguish the two states by adding new indices of “1” or “2” showing “generation” from the left to the right. When we choose the signs of the two bulk masses  $M_F, M'_F$  as  $M_F > 0, M'_F > 0$ , the way of localization of the zero modes is as in Fig. 5. The concrete forms of mode functions for  $\Psi$  are the same in Eq. (17) and we know those for  $\Psi'$  after adding prime symbol ' in some parameters as  $\psi_{1L}^{(0)} \rightarrow \psi'_{1L}{}^{(0)}, \psi_{2L}^{(0)} \rightarrow \psi'_{2L}{}^{(0)}, M_F \rightarrow M'_F, L_1 \rightarrow L'_1$  in Eq. (16).



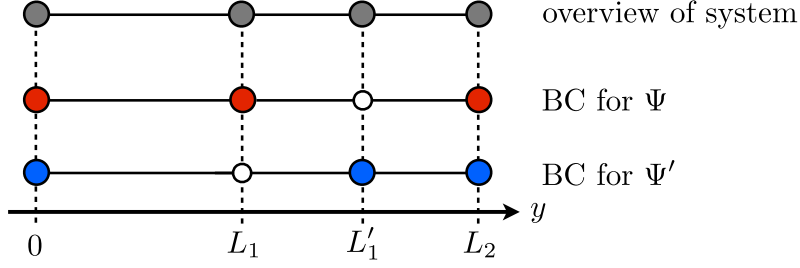


Figure 4: This is an overview of our system with two point interactions, where the red (blue) circular spots show the Dirichlet-type BC for left- (right-) handed part at the corresponding boundary points, respectively, and the small white dots mean the continuous condition for fermions.

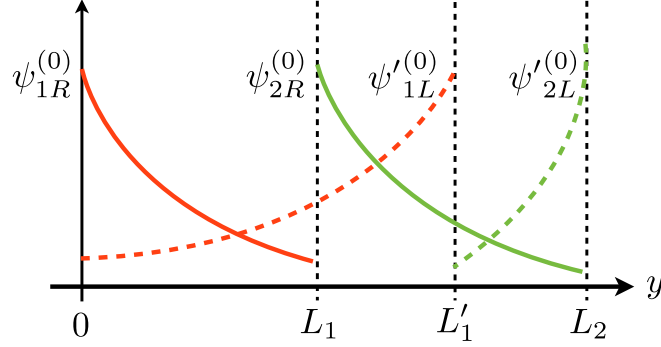


Figure 5: Zero mode profiles of 5D fermions  $\Psi$  and  $\Psi'$ .

The remarkable point in the system with the two point interactions is that the two zero modes with different 4D chirality and “generation” indices overlap in a middle region ( $L_1 < y < L'_1$ ) of the system. This means that flavor mixing can be realized in our configuration. When we consider a UED-type scenario, right- and left-handed fermions are supplied by different 5D fields of  $SU(2)_W$  doublet and singlet, respectively and separately. Thereby we can install this mechanism into UED model with no obstacle. In the SM, in fact, the flavor mixing structure is incorporated in the Yukawa sector with Yukawa couplings with the most general form and three copies of each  $SU(2)_W$  doublet and singlet in the gauge eigenbases. These situations are affected exceedingly after adapting our mechanism for realizing flavor mixing. In addition, we should consider the profile of Higgs because it is a very important ingredient in Yukawa sector. These issues will be discussed concretely in the next section.

### 3 Searching for the possibility for achieving quark mass hierarchy and mixing in multi point interaction system

Based on our discussion in Section 2, we make an attempt to create a model, where quark mass hierarchy and mixing are accomplished by use of the mechanism of flavor mixing due to multi point interactions. In this section, we consider the following form of action  $S$  with effective Yukawa

coupling in new geometry:

$$\begin{aligned}
S = \int d^4x \int_0^{L_3} dy \Bigg\{ & \left[ \bar{Q} (i\partial_M \Gamma^M + M_Q) Q + \bar{\mathcal{U}} (i\partial_M \Gamma^M + M_{\mathcal{U}}) \mathcal{U} \right. \\
& \left. + \bar{\mathcal{D}} (i\partial_M \Gamma^M + M_{\mathcal{D}}) \mathcal{D} \right] \\
& \left. - \left[ Y^{(u)} \bar{\mathcal{U}} \langle \phi(y) \rangle \mathcal{U} + Y^{(d)} \bar{\mathcal{D}} \langle \phi(y) \rangle \mathcal{D} + \text{h.c.} \right] \right\}. \tag{28}
\end{aligned}$$

We have introduced one  $SU(2)_W$  quark doublet  $Q$ , one up-type quark singlet  $\mathcal{U}$ , one down-type quark singlet  $\mathcal{D}$  with their 5D Dirac bulk masses  $M_Q, M_{\mathcal{U}}, M_{\mathcal{D}}$ . We would like to emphasize that our model does not possess any generation index at this stage and that the fermion generation can appear dynamically. Here we have assumed that a ‘‘Higgs doublet’’  $\mathcal{H}$  acquires VEV with  $y$ -position dependence such as

$$\mathcal{H} = \begin{pmatrix} 0 \\ \langle \phi(y) \rangle \end{pmatrix} \tag{29}$$

and that the structure of the Yukawa sector is the same with that of the SM. Note that the 5D up (down) quark Yukawa coupling  $Y^{(u)}$  ( $Y^{(d)}$ ) also do not contain any generation index of the quarks in our model. The  $SU(2)_W$  quark doublet can be decomposed as

$$Q = \begin{pmatrix} U \\ D \end{pmatrix}. \tag{30}$$

Before we go into more details, we would like to point out some remarkable properties of our model. The form of the action in Eq. (28) seems to be very similar to the corresponding part of the mUED model at the first glance. But there are two significant differences between the two theories, as explained below.

One is about the structure of Yukawa coupling. In the UED, we should introduce three copies of fermion configurations to realize the three generation structure of the SM. Profiles of mode functions describing zero mode fermions take constant, therefore the fine-tuning in the Yukawa couplings is inevitable. On the other hand, we only introduce one copy of fermion configurations in our model.

The other one can be seen in properties of the VEV of the Higgs boson. In mUED models, BCs of the Higgs field are chosen as the Neumann-type, then the VEV gets to be a constant, whose situation is the same with the SM. Here we consider the Yukawa structure in our model briefly. As in Eq. (28), the 5D Yukawa couplings do not possess any generation indices. The SM Yukawa structure is expected to be produced through geometry of an effective form of Higgs VEV and the lopsided wave functions of zero mode fermions. In our model, the VEV profile of the Higgs scalar  $\langle \phi \rangle$  is assumed to be  $y$ -position-dependent and to take the ‘‘warped’’ form of

$$\langle \phi(y) \rangle = \mathcal{A} \exp[\alpha(y - L)], \tag{31}$$

with two massive parameters  $\mathcal{A}$  and  $\alpha$ , whose mass dimensions are  $3/2$  and  $1$ , respectively.  $L (= L_3)$  means the length of the total system. The reason for forming this conjecture is that this shape of the VEV is preferable to generate the large quark mass hierarchy in the SM within a natural-ordered setting of parameters. At this stage, we do not worry about the way of realizing this type

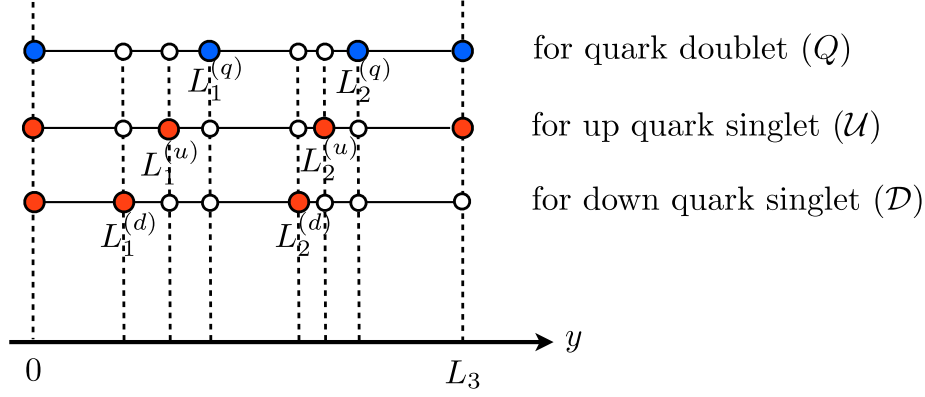


Figure 6: A schematic diagram for explaining our attempt. Conventions of circular spots and dots are the same those in Fig. 4.

of VEV profile and mainly devote our attention to phenomenological issues of it. In a later section, we discuss an example of materializing this (assumed) setup by use of the generalized Higgs BCs discussed in Ref. [60].

We have to introduce new point interactions, where we take the Dirichlet BC, for all of  $Q, \mathcal{U}, \mathcal{D}$  to realize three generations in the SM. To this end, we assume that each 5D fermion feels nontrivially two point interactions with the Dirichlet BC. It turns out that zero modes of the fermions are three-fold degenerate, where each profile is confined in one of three segments. Here we consider the quark profiles explained in Fig. 6, where the meaning of the red and blue circular spots and the white dots are the same with those in Fig. 4. It should be emphasized that the positions of point interactions which each 5D fermion feels are not necessarily common. We assign the coordinates of the lower and upper ends of the total system with  $0 (= L_0)$  and  $L_3$ , respectively, and the locations of point interactions between the two end points of the interval are represented by  $L_1^{(q)}, L_2^{(q)}, L_1^{(u)}, L_2^{(u)}, L_1^{(d)}, L_2^{(d)}$  with the superscripts for identifying the type of the fields and the subscripts for showing the sequences when we count them from the left to the right (see Fig. 6).

Concretely speaking, we adopt the following BCs for  $Q, \mathcal{U}, \mathcal{D}$ , respectively as

$$Q_R = 0 \quad \text{at} \quad y = 0, L_1^{(q)} \pm \varepsilon, L_2^{(q)} \pm \varepsilon, L_3, \quad (32)$$

$$\mathcal{U}_L = 0 \quad \text{at} \quad y = 0, L_1^{(u)} \pm \varepsilon, L_2^{(u)} \pm \varepsilon, L_3, \quad (33)$$

$$\mathcal{D}_L = 0 \quad \text{at} \quad y = 0, L_1^{(d)} \pm \varepsilon, L_2^{(d)} \pm \varepsilon, L_3, \quad (34)$$

where three-fold generated left- (right-) handed zero modes emerge in  $Q (\mathcal{U}, \mathcal{D})$  as we have discussed before. Here we omit to describe the “continuous” condition for each field. It is noted that the profiles of  $U$  and  $D$  get to be the same in our configuration. The orders of the positions are settled on as

$$\begin{aligned} 0 (= L_0) &< L_1^{(u)} < L_1^{(q)} < L_2^{(u)} < L_2^{(q)} < L_3, \\ 0 (= L_0) &< L_1^{(d)} < L_1^{(q)} < L_2^{(d)} < L_2^{(q)} < L_3. \end{aligned} \quad (35)$$

We comment that values of 4D effective Yukawa masses are evaluated as those of overlap integrals among the VEV, right- and left-handed modes. Then both magnitudes and signs of the bulk masses  $M_Q, M_{\mathcal{U}}, M_{\mathcal{D}}$  govern an important part of the results.

The forms of effective 4D Yukawa masses among the three generations are obtained after integration over  $y$  as

$$\begin{aligned}
- \int_0^{L_3} dy \left[ Y^{(u)} \bar{U} \langle \phi(y) \rangle \mathcal{U} + Y^{(d)} \bar{D} \langle \phi(y) \rangle \mathcal{D} + \text{h.c.} \right] = & - \left[ \bar{u}_{1L}^{(0)}(x), \bar{u}_{2L}^{(0)}(x), \bar{u}_{3L}^{(0)}(x) \right] \mathcal{M}^{(u)} \begin{bmatrix} u_{1R}^{(0)} \\ u_{2R}^{(0)} \\ u_{3R}^{(0)} \end{bmatrix} \\
& - \left[ \bar{d}_{1L}^{(0)}(x), \bar{d}_{2L}^{(0)}(x), \bar{d}_{3L}^{(0)}(x) \right] \mathcal{M}^{(d)} \begin{bmatrix} d_{1R}^{(0)} \\ d_{2R}^{(0)} \\ d_{3R}^{(0)} \end{bmatrix} + \text{h.c.},
\end{aligned} \tag{36}$$

where the mass matrices  $\mathcal{M}^{(u)}$  and  $\mathcal{M}^{(d)}$  have the following structure

$$\mathcal{M}^{(u)} = \begin{bmatrix} m_{11}^{(u)} & m_{12}^{(u)} & 0 \\ 0 & m_{22}^{(u)} & m_{21}^{(u)} \\ 0 & 0 & m_{33}^{(u)} \end{bmatrix}, \quad \mathcal{M}^{(d)} = \begin{bmatrix} m_{11}^{(d)} & m_{12}^{(d)} & 0 \\ 0 & m_{22}^{(d)} & m_{21}^{(d)} \\ 0 & 0 & m_{33}^{(d)} \end{bmatrix}. \tag{37}$$

The three-fold degenerated zero modes are distinguished by the generation indices “1, 2, 3” in both up-type quarks ( $u$ ) and down-type ones ( $d$ ). Each matrix component in Eq. (37) is calculated by overlap integrals among the Higgs VEV and zero mode functions of right- and left-handed fermions, which are functions of the fermion bulk masses  $M_Q, M_U, M_D$  and the locations of the point interactions  $L_1^{(q)}, L_2^{(q)}, L_1^{(u)}, L_2^{(u)}, L_1^{(d)}, L_2^{(d)}$ . In contrast to the SM, some elements of the Yukawa mass matrices are zero. The diagonal parts of  $m_{11}^{(u)}, m_{22}^{(u)}, m_{33}^{(u)}, m_{11}^{(d)}, m_{22}^{(d)}, m_{33}^{(d)}$  are always nonzero unless we take an extremal parameter choice, *e.g.*,  $L_1^{(u)} = L_2^{(u)}$ , which, of course, is unsuitable for our purpose in this paper. We notice that the characteristic form of the mass matrices in Eq. (37) is given by the geometry of our setting. Some of the components in the mass matrices vanish due to no overlapping of mode functions.

Which non-diagonal component is nonzero depends on the positions of the point interactions. Following the rule in Eq. (35), the only (1, 2) and (2, 3) elements are nonzero. When we reverse the order of position between  $L_1^{(q)}$  and  $L_1^{(u)}$  as

$$L_1^{(u)} < L_1^{(q)} \rightarrow L_1^{(q)} < L_1^{(u)}, \tag{38}$$

the value of the (1, 2) component vanishes ( $m_{12}^{(u)} = 0$ ) but that of the (2, 1) component becomes nonzero ( $m_{21}^{(u)} \neq 0$ ). This issue is easily understandable when we focus on the fact that the row (column) index of the mass matrix corresponds to the generation of the left- (right-) handed fermion, respectively. We would like to mention that in our model, flavor mixing is inevitable to realize the SM quark masses. Because in the aligned configuration of  $L_1^{(q)} = L_1^{(u)} = L_1^{(d)}$ ,  $L_2^{(q)} = L_2^{(u)} = L_2^{(d)}$ , it is very hard to realize the quark mass patterns of the first generation ( $m_{\text{up}} < m_{\text{down}}$ ) and those of the third generation ( $m_{\text{top}} > m_{\text{bottom}}$ ) simultaneously.

The point is whether we can reproduce the structure of the CKM matrix or not based on the limited forms of the Yukawa mass matrices, where we never find the overlapping between first and third generations. After some calculations, we can find a set of input parameters where we reproduce the quark mass hierarchy and the CKM matrix simultaneously. In the next subsection, we discuss, in detail, whether we can simultaneously reproduce the structure of the quark mass hierarchy and the CKM matrix based on the limited forms of the Yukawa mass matrices (37) without the overlapping between the first and third generations.

### 3.1 A solution in the setup with a warped VEV

Let us first give the concrete forms of the Yukawa mass matrices in our system which have been discussed in the previous subsection. The fields  $Q, \mathcal{U}, \mathcal{D}$  with the BCs in Eqs (32), (33) and (34) are KK-decomposed as follows:

$$Q(x, y) = \begin{pmatrix} U(x, y) \\ D(x, y) \end{pmatrix} = \begin{pmatrix} \sum_{i=1}^3 u_{iL}^{(0)}(x) f_{q_{iL}}^{(0)}(y) \\ \sum_{i=1}^3 d_{iL}^{(0)}(x) f_{q_{iL}}^{(0)}(y) \end{pmatrix} + (\text{KK modes}), \quad (39)$$

$$\mathcal{U}(x, y) = \sum_{i=1}^3 u_{iR}^{(0)}(x) f_{u_{iR}}^{(0)}(y) + (\text{KK modes}), \quad (40)$$

$$\mathcal{D}(x, y) = \sum_{i=1}^3 d_{iR}^{(0)}(x) f_{d_{iR}}^{(0)}(y) + (\text{KK modes}), \quad (41)$$

where we only focus on the zero mode parts. Here the zero mode functions are obtained in the following forms

$$f_{q_{iL}}^{(0)}(y) = \mathcal{N}_i^{(q)} e^{M_Q(y-L_{i-1}^{(q)})} \left[ \theta(y - L_{i-1}^{(q)}) \theta(L_i^{(q)} - y) \right], \quad (42)$$

$$f_{u_{iR}}^{(0)}(y) = \mathcal{N}_i^{(u)} e^{-M_{\mathcal{U}}(y-L_{i-1}^{(u)})} \left[ \theta(y - L_{i-1}^{(u)}) \theta(L_i^{(u)} - y) \right], \quad (43)$$

$$f_{d_{iR}}^{(0)}(y) = \mathcal{N}_i^{(d)} e^{-M_{\mathcal{D}}(y-L_{i-1}^{(d)})} \left[ \theta(y - L_{i-1}^{(d)}) \theta(L_i^{(d)} - y) \right], \quad (44)$$

where we use the conventions, for clarity, of

$$\begin{aligned} \Delta L_i^{(l)} &= L_i^{(l)} - L_{i-1}^{(l)} \quad (\text{for } i = 1, 2, 3; \ l = q, u, d), \\ 0 (= L_0) &= L_0^{(q)} = L_0^{(u)} = L_0^{(d)}, \\ L_3 &= L_3^{(q)} = L_3^{(u)} = L_3^{(d)}, \end{aligned}$$

$$\mathcal{N}_i^{(q)} = \sqrt{\frac{2M_Q}{e^{2M_Q \Delta L_i^{(q)}} - 1}}, \quad \mathcal{N}_i^{(u)} = \sqrt{\frac{2M_{\mathcal{U}}}{1 - e^{-2M_{\mathcal{U}} \Delta L_i^{(u)}}}}, \quad \mathcal{N}_i^{(d)} = \sqrt{\frac{2M_{\mathcal{D}}}{1 - e^{-2M_{\mathcal{D}} \Delta L_i^{(d)}}}}. \quad (45)$$

$\mathcal{N}_i^{(q)}, \mathcal{N}_i^{(u)}, \mathcal{N}_i^{(d)}$  are wavefunction normalization factors for  $f_{q_{iL}}^{(0)}, f_{u_{iR}}^{(0)}, f_{d_{iR}}^{(0)}$ , respectively. The length of the total system  $L$  takes the universal value of

$$L := L_3 = L_3^{(q)} - L_0^{(q)} = L_3^{(u)} - L_0^{(u)} = L_3^{(d)} - L_0^{(d)}. \quad (46)$$

Here we choose the signs of the fermion bulk masses  $M_Q, M_{\mathcal{U}}, M_{\mathcal{D}}$  as

$$M_Q > 0, M_{\mathcal{U}} < 0, M_{\mathcal{D}} > 0, \quad (47)$$

where we take a negative value in  $M_{\mathcal{U}}$  to generate a large overlapping for the top quark mass (mainly) in  $m_{33}^{(u)}$ . An outlines of the wavefunction profiles are summarized in Fig. 7.

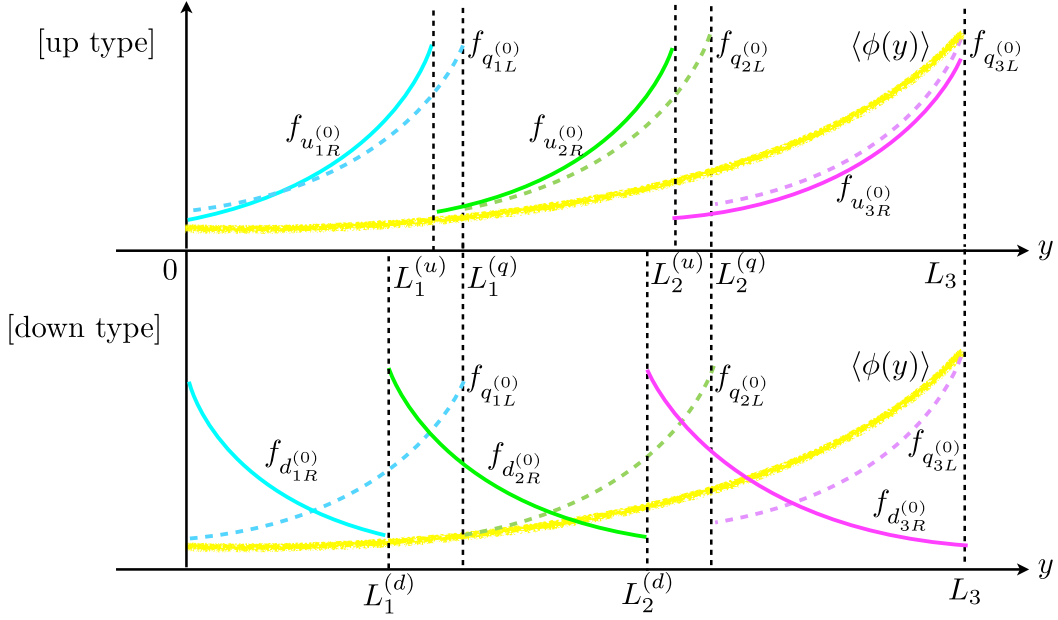


Figure 7: An outlines of the wavefunctions profiles.

Each component of the  $\mathcal{M}^{(u)}$  and  $\mathcal{M}^{(d)}$  is acquired by calculating the corresponding overlap integral as follows:

$$\begin{aligned}
 m_{11}^{(u)} &= Y^{(u)} \int_0^{L_1^{(u)}} dy f_{q_{1L}}^{(0)}(y) f_{u_{1R}}^{(0)}(y) \langle \phi(y) \rangle \\
 &= \mathcal{N}_1^{(q)} \mathcal{N}_1^{(u)} Y^{(u)} \mathcal{A} e^{-\alpha L} \left\{ \frac{e^{(M_Q + |M_U| + \alpha)L_1^{(u)}} - 1}{M_Q + |M_U| + \alpha} \right\}, \tag{48}
 \end{aligned}$$

$$\begin{aligned}
 m_{22}^{(u)} &= Y^{(u)} \int_{L_1^{(q)}}^{L_2^{(u)}} dy f_{q_{2L}}^{(0)}(y) f_{u_{2R}}^{(0)}(y) \langle \phi(y) \rangle \\
 &= \mathcal{N}_2^{(q)} \mathcal{N}_2^{(u)} Y^{(u)} \mathcal{A} e^{-\alpha L} \left\{ \frac{e^{(M_Q + |M_U| + \alpha)L_2^{(u)}} - e^{(M_Q + |M_U| + \alpha)L_1^{(q)}}}{M_Q + |M_U| + \alpha} \right\} e^{-M_Q L_1^{(q)} - |M_U| L_1^{(u)}}, \tag{49}
 \end{aligned}$$

$$\begin{aligned}
 m_{33}^{(u)} &= Y^{(u)} \int_{L_2^{(q)}}^{L_3^{(q)}} dy f_{q_{3L}}^{(0)}(y) f_{u_{3R}}^{(0)}(y) \langle \phi(y) \rangle \\
 &= \mathcal{N}_3^{(q)} \mathcal{N}_3^{(u)} Y^{(u)} \mathcal{A} e^{-\alpha L} \left\{ \frac{e^{(M_Q + |M_U| + \alpha)L_3^{(q)}} - e^{(M_Q + |M_U| + \alpha)L_2^{(q)}}}{M_Q + |M_U| + \alpha} \right\} e^{-M_Q L_2^{(q)} - |M_U| L_2^{(u)}}, \tag{50}
 \end{aligned}$$

$$\begin{aligned}
m_{12}^{(u)} &= Y^{(u)} \int_{L_1^{(u)}}^{L_1^{(q)}} dy f_{q_{1L}^{(0)}}(y) f_{u_{2R}^{(0)}}(y) \langle \phi(y) \rangle \\
&= \mathcal{N}_1^{(q)} \mathcal{N}_2^{(u)} Y^{(u)} \mathcal{A} e^{-\alpha L} \left\{ \frac{e^{(M_Q + |M_U| + \alpha)L_1^{(q)}} - e^{(M_Q + |M_U| + \alpha)L_1^{(u)}}}{M_Q + |M_U| + \alpha} \right\} e^{-|M_U|L_1^{(u)}}, \tag{51}
\end{aligned}$$

$$\begin{aligned}
m_{23}^{(u)} &= Y^{(u)} \int_{L_2^{(u)}}^{L_2^{(q)}} dy f_{q_{2L}^{(0)}}(y) f_{u_{3R}^{(0)}}(y) \langle \phi(y) \rangle \\
&= \mathcal{N}_2^{(q)} \mathcal{N}_3^{(u)} Y^{(u)} \mathcal{A} e^{-\alpha L} \left\{ \frac{e^{(M_Q + |M_U| + \alpha)L_2^{(q)}} - e^{(M_Q + |M_U| + \alpha)L_2^{(u)}}}{M_Q + |M_U| + \alpha} \right\} e^{-M_Q L_1^{(q)} - |M_U|L_2^{(u)}}, \tag{52}
\end{aligned}$$

$$\begin{aligned}
m_{11}^{(d)} &= Y^{(d)} \int_0^{L_1^{(d)}} dy f_{q_{1L}^{(0)}}(y) f_{d_{1R}^{(0)}}(y) \langle \phi(y) \rangle \\
&= \mathcal{N}_1^{(q)} \mathcal{N}_1^{(d)} Y^{(d)} \mathcal{A} e^{-\alpha L} \left\{ \frac{e^{(M_Q - M_D + \alpha)L_1^{(d)}} - 1}{M_Q - M_D + \alpha} \right\}, \tag{53}
\end{aligned}$$

$$\begin{aligned}
m_{22}^{(d)} &= Y^{(d)} \int_{L_1^{(q)}}^{L_2^{(d)}} dy f_{q_{2L}^{(0)}}(y) f_{d_{2R}^{(0)}}(y) \langle \phi(y) \rangle \\
&= \mathcal{N}_2^{(q)} \mathcal{N}_2^{(d)} Y^{(d)} \mathcal{A} e^{-\alpha L} \left\{ \frac{e^{(M_Q - M_D + \alpha)L_2^{(d)}} - e^{(M_Q - M_D + \alpha)L_1^{(q)}}}{M_Q - M_D + \alpha} \right\} e^{-M_Q L_1^{(q)} + M_D L_1^{(d)}}, \tag{54}
\end{aligned}$$

$$\begin{aligned}
m_{33}^{(d)} &= Y^{(d)} \int_{L_2^{(q)}}^{L_3^{(d)}} dy f_{q_{3L}^{(0)}}(y) f_{d_{3R}^{(0)}}(y) \langle \phi(y) \rangle \\
&= \mathcal{N}_3^{(q)} \mathcal{N}_3^{(d)} Y^{(d)} \mathcal{A} e^{-\alpha L} \left\{ \frac{e^{(M_Q - M_D + \alpha)L_3^{(d)}} - e^{(M_Q - M_D + \alpha)L_2^{(q)}}}{M_Q - M_D + \alpha} \right\} e^{-M_Q L_2^{(q)} + M_D L_2^{(d)}}, \tag{55}
\end{aligned}$$

$$\begin{aligned}
m_{12}^{(d)} &= Y^{(d)} \int_{L_1^{(d)}}^{L_1^{(q)}} dy f_{q_{1L}^{(0)}}(y) f_{d_{2R}^{(0)}}(y) \langle \phi(y) \rangle \\
&= \mathcal{N}_1^{(q)} \mathcal{N}_2^{(d)} Y^{(d)} \mathcal{A} e^{-\alpha L} \left\{ \frac{e^{(M_Q - M_D + \alpha)L_1^{(q)}} - e^{(M_Q - M_D + \alpha)L_1^{(d)}}}{M_Q - M_D + \alpha} \right\} e^{M_D L_1^{(d)}}, \tag{56}
\end{aligned}$$

$$\begin{aligned}
m_{23}^{(d)} &= Y^{(d)} \int_{L_2^{(d)}}^{L_2^{(q)}} dy f_{q_{2L}^{(0)}}(y) f_{d_{3R}^{(0)}}(y) \langle \phi(y) \rangle \\
&= \mathcal{N}_2^{(q)} \mathcal{N}_3^{(d)} Y^{(d)} \mathcal{A} e^{-\alpha L} \left\{ \frac{e^{(M_Q - M_D + \alpha)L_2^{(q)}} - e^{(M_Q - M_D + \alpha)L_2^{(d)}}}{M_Q - M_D + \alpha} \right\} e^{-M_Q L_1^{(q)} + M_D L_2^{(d)}}, \tag{57}
\end{aligned}$$

where we have used the forms of wavefunctions in Eqs. (42), (43), (44), the conventions in Eq. (45), and the assumed profiles of the Higgs VEV in Eq. (31). In this paper, we choose the parameters

up quark	mass	down quark	mass
up ( $u$ )	1.8-3.0 MeV	down ( $d$ )	4.5-5.5 MeV
charm ( $c$ )	1.250-1.300 GeV	strange ( $s$ )	90-100 MeV
top ( $t$ )	172.1-174.9 GeV	bottom ( $b$ )	4.15-4.21 GeV

Table 1: Experimental values of quark masses from Ref. [61].

as

$$\begin{aligned}
L_1^{(q)} &= 0.338 \cdot L, & L_2^{(q)} &= 0.689 \cdot L, & L_3^{(q)} &= 1 \cdot L, \\
L_1^{(u)} &= 0.0115 \cdot L, & L_2^{(u)} &= 0.540 \cdot L, & L_3^{(u)} &= 1 \cdot L, \\
L_1^{(d)} &= 0.223 \cdot L, & L_2^{(d)} &= 0.676 \cdot L, & L_3^{(d)} &= 1 \cdot L, \\
M_Q &= 6.67 \cdot L^{-1}, & M_{\mathcal{U}} &= -7.98 \cdot L^{-1}, & M_{\mathcal{D}} &= 6.16 \cdot L^{-1}, \\
\alpha &= 8.67 \cdot L^{-1}, & Y^{(u)}/Y^{(d)} &= 12.0, & \mathcal{A}Y^{(u)} &= 275 \text{ GeV},
\end{aligned} \tag{58}$$

which reproduce the quark mass hierarchy and the CKM matrix with a good precision. The quark mass eigenvalues and the CKM matrix are evaluated from Eqs.(48)–(57). The diagonalized Yukawa mass matrices take the forms of

$$\mathcal{M}^{(u)}|_{\text{diagonal}} = \text{diag} (2.13 \text{ MeV}, 1.18 \text{ GeV}, 174 \text{ GeV}), \tag{59}$$

$$\mathcal{M}^{(d)}|_{\text{diagonal}} = \text{diag} (3.85 \text{ MeV}, 110 \text{ MeV}, 4.19 \text{ GeV}), \tag{60}$$

and the CKM matrix is given as

$$|V_{\text{CKM}}| = \begin{bmatrix} 0.976 & 0.213 & 0.00448 \\ 0.213 & 0.976 & 0.0475 \\ 0.0145 & 0.0454 & 0.999 \end{bmatrix}. \tag{61}$$

Subsequently, we present the latest experimental values. The quark masses are summarized in Table 1 and the CKM matrix is

$$|V_{\text{CKM}}|_{\text{exp.}} = \begin{bmatrix} 0.974 & 0.225 & 0.00415 \\ 0.230 & 1.006 & 0.0409 \\ 0.0084 & 0.0429 & 0.89 \end{bmatrix} \tag{62}$$

from Ref. [61]. From the results in Eqs. (59) and (60), the mass eigenvalues are well reproduced within about twenty percent differences and the absolute values of the CKM matrix elements are also described within about twenty percent differences in almost all the elements. But we should comment on the  $(3, 1)$  component of the CKM matrix which we have obtained, where the deviation ratio measures up to  $\sim 70\%$ .

At this stage, we ponder over the number of the input parameters and constraints originated from the equations. After keeping the relations about the positions in Eqs. (45) and (46) in mind, we count the independent d.o.f. (degrees of freedom) as 7 for the positions of boundary points, 3 for fermion bulk masses, 2 for 5D Yukawa couplings, 2 for effective Higgs VEV parameters, respectively, and the total d.o.f. is 14. Meanwhile, the total number of the constraints is 9, where they consist of 6 quark mass eigenvalues and 3 CKM mixing angles. Here the two massive parameters of

$$Y^{(u)} \text{ (or } Y^{(d)}, \mathcal{A}), L \tag{63}$$



are still not specified. It is noted that once one of  $Y^{(u)}, Y^{(d)}, \mathcal{A}$  is fixed, the other is determined simultaneously. The reason for this indetermination is that the electroweak scale is not indicated within our analysis.

The results in Eq. (58) are realized broadly within  $\mathcal{O}(10)$  range (when we choose the basis of scaling as  $L^{-1}$ ) and it is shown that we can explain both of the quark mass hierarchy and the structure of the CKM matrix in a natural statement.

## 4 An example for realizing warped Higgs VEV by generalized Higgs boundary condition

In the previous section, we have verified the possibility of accomplishing the quark mass hierarchy and the structure of the CKM matrix at the same instant without fine-tuning of parameters in the setup, whose geometry contains many point interactions. Here we have assumed the forms of 5D Yukawa couplings and the warped shape of the Higgs VEV profile  $\langle\phi(y)\rangle$ . In this section, we give an example of generating this situation without conflicting with the physics at the SM.

### 4.1 Generalized boundary condition for a scalar

Following [60], we can consider the physics which is described by the 5D actions on a single interval  $[0, L]$  for a 5D scalar  $\Phi$  of

$$S_\Phi = \int d^4x \int_0^L dy \left\{ \Phi^\dagger \partial^\mu \partial_\mu \Phi + \Phi^\dagger \partial_y^2 \Phi - V(|\Phi|^2) \right\}, \quad (64)$$

with the bulk potential  $V(|\Phi|^2) = M^2 |\Phi|^2 + \frac{\lambda}{2} |\Phi|^4$  and where we do not consider tree level brane-localized term. The parameters  $M^2, \lambda$  need to be real due to hermiticity. We can find a difference from the ordinary UED-type form in the structure of the derivatives. Based on variational principle, the following form should vanish at the boundaries  $y = 0, L$ :

$$\Phi^\dagger \partial_y \delta \Phi - (\partial_y \Phi)^\dagger \delta \Phi = 0 \quad \text{at } y = 0, L. \quad (65)$$

It turns out that a larger class of BCs is allowed with two new real massive parameters  $L_\pm$ , whose mass dimensions are  $-1$ , as

$$\begin{aligned} \Phi + L_+ \partial_y \Phi &= 0 & \text{at } y &= 0, \\ \Phi - L_- \partial_y \Phi &= 0 & \text{at } y &= L, \end{aligned} \quad (66)$$

where  $L_\pm$  can take values in the range of  $-\infty \leq L_\pm \leq \infty$ . This type of BC is called Robin boundary condition. It is obvious that the above conditions include the ordinary Neumann (Dirichlet) BC in the case of  $L_\pm = \pm\infty$  ( $L_\pm = 0$ ).

### 4.2 Position-dependent scalar VEV in generalized boundary condition

In this subsection, we discuss the profile of the scalar singlet  $\Phi$  and its phase structure. In the mUED model, where the Higgs doublet takes the Neumann BC at the both boundaries, the 4D

effective Higgs potential is minimized with ease, where the VEV is a constant ( $y$ -independent) and the situation is the same with the SM.

On the other hand in our model, the phase structure is nontrivial because the massive parameters  $L_{\pm}$  emerge in our generalized BC in Eq. (66). To investigate properties of phase structure of the scalar  $\Phi$ , we have to solve the minimization problem of the functional indicating 4D effective Higgs potential

$$\mathcal{E}[\Phi] := \int_0^L dy \left\{ -\Phi^\dagger \partial_y^2 \Phi + V(|\Phi|^2) \right\} = \int_0^L dy \left\{ -\Phi^\dagger \partial_y^2 \Phi + M^2 |\Phi|^2 + \frac{\lambda}{2} |\Phi|^4 \right\}. \quad (67)$$

It is important to incorporate the kinetic term along the extra spacial direction into the potential because the minimum configuration of the singlet  $\Phi$  probably possesses  $y$ -dependence, as we will see below.

Hereafter we search for the form of the VEV  $\langle \Phi(y) \rangle$  by solving the EOM

$$(-\partial_y^2 + M^2)\Phi + \lambda \Phi^\dagger \Phi^2 = 0, \quad (68)$$

which can be obtained after taking variation in Eq. (67). The solutions of Eq. (68) are found to be expressed in terms of the Jacobi's elliptic functions generally. The types of solutions with  $M^2 > 0$  are classified based on a parameter  $Q$ , which is an integration constant after integrating along  $y$ , with mass dimensions 5. It turns out that with the choice of  $Q < 0$  a solution of Eq. (68), which can realize a desired “warped” VEV in an asymptotic form, is give by

$$\langle \Phi(y) \rangle = \nu \cdot \frac{1}{\text{cn} \left( \sqrt{\frac{\lambda}{2}} \frac{\mu}{k} (y - y_0), k \right)}, \quad (69)$$

where the several parameters are defined as

$$\mu^2 = \frac{M^2}{\lambda} \left( 1 + \sqrt{1 + \frac{4\lambda|Q|}{M^4}} \right), \quad (70)$$

$$\nu^2 = \frac{M^2}{\lambda} \left( \sqrt{1 + \frac{4\lambda|Q|}{M^4}} - 1 \right), \quad (71)$$

$$k^2 = \frac{\mu^2}{\mu^2 + \nu^2}. \quad (72)$$

$y_0$  means a translation d.o.f. along  $y$ , which appears after integration for solving the equation in (68). The index  $k$  is an important parameter of elliptic function to determine the profile. We can rewrite  $k$  by use of the input parameters in  $\mu, \nu$  as

$$k = \sqrt{\frac{1}{2} \left( 1 + \frac{1}{\sqrt{1+X}} \right)} \quad \left( X := \frac{4\lambda|Q|}{M^4} \right), \quad (73)$$

where we conclude that the possible region of the value of  $k$  is

$$\sqrt{\frac{1}{2}} \leq k \leq 1. \quad (74)$$

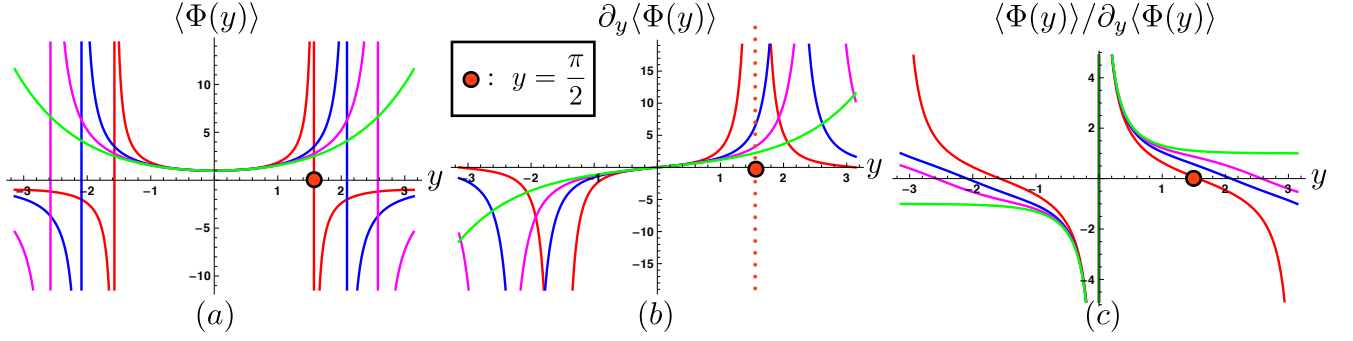


Figure 8: These three plots represent the VEV profile of  $\langle \Phi(y) \rangle = 1/\text{cn}(y, k)$  in (a), its first derivative  $\partial_y \langle \Phi(y) \rangle$  in (b) and the form of  $\langle \Phi(y) \rangle / \partial_y \langle \Phi(y) \rangle$  in (c). The red, blue, magenta, green curves are in  $k = 0, 0.71, 0.9, 1$ , respectively. The red dots are the points of  $y = \pi/2$ .

Here we mention that the condition  $\lambda > 0$  is required to ensuring the stability of the vacuum. We again write down the form of  $\Phi$  with less abbreviation:

$$\langle \Phi(y) \rangle = \left[ \frac{M}{\sqrt{\lambda}} \left\{ \sqrt{1+X} - 1 \right\}^{1/2} \right] \times \frac{1}{\text{cn} \left( M \{1+X\}^{1/4} (y - y_0), \sqrt{\frac{1}{2} \left( 1 + \frac{1}{\sqrt{1+X}} \right)} \right)}. \quad (75)$$

Next we decide to choose our strategy to treat scalar BC. We rewrite Eq. (66) as follows:

$$L_+ = - \langle \Phi(0) \rangle / \partial_y \langle \Phi(0) \rangle, \quad L_- = + \langle \Phi(L) \rangle / \partial_y \langle \Phi(L) \rangle. \quad (76)$$

The  $L_+, L_-$  are determined by the values of  $\langle \Phi(y) \rangle, \partial_y \langle \Phi(y) \rangle$  at the endpoints  $y = 0, L$  and we discuss the shapes of  $\langle \Phi(y) \rangle, \partial_y \langle \Phi(y) \rangle$  at first. In Fig. 8, we show three plots of  $\langle \Phi(y) \rangle, \partial_y \langle \Phi(y) \rangle$  and  $\langle \Phi(y) \rangle / \partial_y \langle \Phi(y) \rangle$ , with suitable normalizations. The red, blue, magenta, green curves are in  $k = 0, 0.71, 0.9, 1$ , respectively and the red dots are the points of  $y = \pi/2$ . We give some comments in order.

- The function of  $1/\text{cn}(y)$  can be represented as trigonometric or hyperbolic function in extremal cases of  $k$ , concretely, which is  $1/\text{cn}(y)|_{k=0} = 1/\cos(y)$  and  $1/\text{cn}(y)|_{k=1} = \cosh(y)$ . Following the change of the value of  $k$  from 0 to 1, the profile of  $1/\text{cn}(y)$  smoothly shift from  $1/\cos(y)$  to  $\cosh(y)$ .
- $\langle \Phi(y) \rangle|_{k=0}$  and  $\partial_y \langle \Phi(y) \rangle|_{k=0}$  are divergent at  $y = \pi/2$ . Increasing the value of  $k$  from 0 to 1, this divergent point moves from  $\pi/2$  to infinity.
- The profile of  $[\langle \Phi(y) \rangle / \partial_y \langle \Phi(y) \rangle]|_{k=0}$  is divergent at  $y = \pi$  and takes zero value at  $y = \pi/2$ . As increasing the value of  $k$  from 0 to 1, these points move from  $\pi (\pi/2)$  to infinity. This profile is also divergent at  $y = 0$  independently of the value of  $k$ .
- In the region between  $y = 0$  and  $y = y_d$ , where  $y_d$  is a first divergent point with positive value and, of course,  $y_d = \pi/2$  in case of  $k = 0$ . The profile of  $\langle \Phi(y) \rangle / \partial_y \langle \Phi(y) \rangle$  is monotonically decreasing independently of the value of  $k$ .

In this paper, we focus on the segment of  $(0, y_d)$ . At this segment, as we review above, the profile of  $\langle \Phi(y) \rangle / \partial_y \langle \Phi(y) \rangle$  is monotonically decreasing independently of the value of  $k$  and takes positive

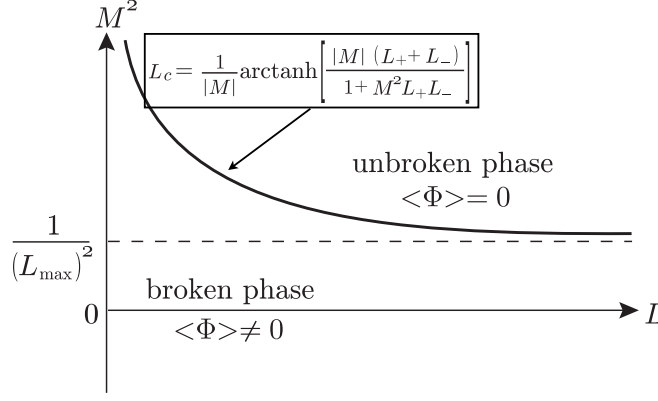


Figure 9: Phase diagram of the scalar  $\Phi$  in the case of  $L_+L_- < 0, L_+ + L_- \leq 0$  in Ref. [60].

value. Therefore, the values of  $L_+, L_-$  obey the following condition:

$$\begin{cases} L_+ < 0 \\ L_- > 0 \\ |L_+| > |L_-| \end{cases}, \quad (77)$$

where the condition,  $L_+ + L_- < 0$ , is automatically derived from the conditions of Eq. (77). The phase structure of the scalar singlet  $\Phi$  with the generalized BC is explored in Ref. [60] and we quote a phase diagram in our case of  $L_+L_- < 0, L_+ + L_- \leq 0$  as Fig. 9.  $L_{\max}$  in Fig. 9 is defined as

$$L_{\max} := \max \{L_+, L_-\} = L_-. \quad (78)$$

The important point is the existence of a critical length  $L_c$  in the region of  $M^2 > 1/L_{\max}^2$ , whose definition is

$$L_c = \frac{1}{|M|} \operatorname{arctanh} \left( \frac{|M|(L_+ + L_-)}{1 + M^2 L_+ L_-} \right) \quad \text{for } M^2 > \frac{1}{L_{\max}^2}, \quad (79)$$

and when we introduce a  $U(1)$  gauge boson, the gauge symmetry is broken (unbroken) for  $L < L_c$  ( $L \geq L_c$ ). On the other hand, the gauge symmetry is always broken in the region of  $M^2 \leq \frac{1}{L_{\max}^2}$ .

Now we discuss properties of the solution. On the condition of

$$k \sim 1 \quad \text{and} \quad -\sqrt{\frac{\lambda}{2}} \frac{\mu}{k} y_0 \gg 1, \quad (80)$$

the form of the solution gets to be exponential as follows:

$$\langle \Phi(y) \rangle \underset{k \sim 1}{\sim} \nu \cosh \left( \sqrt{\frac{\lambda}{2}} \mu (y - y_0) \right) \underset{\sqrt{\frac{\lambda}{2}} \mu (y - y_0) \gg 1}{\sim} \frac{\nu}{2} e^{-\sqrt{\frac{\lambda}{2}} \mu y_0} \cdot e^{\sqrt{\frac{\lambda}{2}} \mu y}, \quad (81)$$

which is just the form of the warped VEV. The detailed analysis including numerical calculation is executed in the subsection 4.4. For more concrete understanding, we go for another analysis, which is based on the discussion in Ref. [60]. We introduce the eigenfunctions  $f_{(n)}(y)$  of the eigenvalue equation

$$-\partial_y^2 f_{(n)}(y) = E_{(n)} f_{(n)}(y), \quad n = 0, 1, 2, \dots, \quad (82)$$

with the BC's

$$f_{(n)}(0) + L_+ \partial_y f_{(n)}(0) = f_{(n)}(L) - L_- \partial_y f_{(n)}(L) = 0. \quad (83)$$

In terms of the orthonormal eigenfunctions  $f_{(n)}(y)$ , whose orthonormality is ensured by the hermiticity of the operator  $(-\partial_y^2)$ , the field  $\Phi$  can be expanded as

$$\Phi(y) = \sum_{n=0}^{\infty} \phi_{(n)} f_{(n)}(y), \quad (84)$$

with the corresponding coefficients  $\phi_{(n)}$ . Inserting it into  $\mathcal{E}[\Phi]$  in Eq. (67) leads to

$$\mathcal{E}[\Phi] = \sum_{n=0}^{\infty} m_{(n)}^2 |\phi_{(n)}|^2 + (\text{quartic terms in } \phi_{(n)}), \quad (85)$$

where

$$m_{(n)}^2 := M^2 + E_{(n)}, \quad n = 0, 1, 2, \dots. \quad (86)$$

Note that the quartic terms are non-negative for any configurations of  $\phi_{(n)}$  because they come from the term of  $\int_0^L dy \frac{\lambda}{2} |\Phi|^4$  ( $\geq 0$ ). It follows that the configuration of the VEV is given by  $\langle \Phi \rangle = 0$  (or  $\langle \phi_{(n)} \rangle = 0$  for any  $n$ ) if  $m_{(n)}^2 \geq 0$  for any  $n$ . For realizing symmetry breaking, the condition  $m_{(0)}^2 < 0$  is mandatory and the  $|\phi_{(0)}|^2$  term's contribution is probably dominant around the minima.<sup>4</sup> Consequently, we could approximate the form of  $\langle \Phi(y) \rangle$  as

$$\langle \Phi(y) \rangle \sim \phi_{(0)} f_{(0)}(y). \quad (87)$$

Here we take the two parameters of the BC as

$$\frac{1}{L_{\pm}} = \mp (M + \epsilon), \quad (88)$$

where  $\epsilon$  is an microscopic (but not infinitesimal) and positive value. It is not difficult to obtain the form of  $f_{(0)}(y)$  and the corresponding eigenvalue  $E_{(0)}$  with the assumptions

$$f_{(0)}(y) \sim e^{(M+\epsilon)y}, \quad E_{(0)} = -(M + \epsilon)^2, \quad (89)$$

where we derive the form of the warped VEV again. By calculating the value of  $m_{(0)}$  as

$$m_{(0)}^2 = -2\epsilon M - \epsilon^2, \quad (90)$$

we can infer that the symmetry breaking is realized for a certainty with our premise of  $M > 0$ .<sup>5</sup>

---

<sup>4</sup> Continuing discussions in this way, we can classify the phase structure of the scalar without knowing the details of the VEV  $\langle \Phi \rangle$ .

<sup>5</sup> In other words, the condition  $M^2 < 1/L_{\max}^2$  is fulfilled.

### 4.3 A model for realizing our mechanism without violating gauge universality in multi point interaction system

Now we know that the form of the warped VEV can be achieved by the scalar with the generalized BC in Eq. (66). Naively thinking, in the UED-type model with one Higgs  $SU(2)_W$  doublet  $H$  with the generalized BCs at the two end point of the total system ( $y = 0, y = L$ ), and the “continuous” conditions at the others, we can explain the quark mass hierarchy and the structure of the CKM matrix simultaneously via geometry. But two nontrivial issues exist in this setup.

In the SM, the profile of the VEV  $\langle H \rangle$  can be rotated by use of the  $SU(2)_W$  global symmetry as

$$\langle H \rangle \rightarrow \begin{pmatrix} 0 \\ v/\sqrt{2L} \end{pmatrix}, \quad (91)$$

with  $v = 246 \text{ GeV}$  because the profile  $\langle H \rangle$  is constant. The first issue is that whether we can rotate the profile and obtain the above form or not. In our case the VEV becomes  $y$ -dependent generally and the 4D effective Higgs potential in Eq. (67) is considered to hold a very complicated structure. Thus it is nontrivial that whether the VEV  $\langle H \rangle$  can take the form in Eq. (91).

The second issue is very critical and important. When the VEV is  $y$ -position dependent, zero mode profile of a 4D gauge boson is determined by a Lamé-type equation and is not constant any longer. Then the overlap integrals for quark-antiquark-gauge boson interactions in the SM become generation-dependent and as a consequence, the gauge universality in the SM is jeopardized. Of course this result is unacceptable and thereby we need to alter our strategy.

A remedy for this plague orders the coexistence of a Higgs doublet  $H$  and a singlet scalar  $\Phi$ , where the BC of the former is chosen as the ordinary Neumann-type at the end points as

$$\partial_y H|_{y=0} = \partial_y H|_{y=L} = 0, \quad (92)$$

and of the latter is selected as the generalized BC in Eq. (66). The 5D actions for  $H$  and  $\Phi$  are given as

$$S_H = \int d^4x \int_0^L dy \left\{ H^\dagger (D_M D^M + M'^2) H - \frac{\lambda'}{2} (H^\dagger H)^2 \right\}, \quad (93)$$

$$S_\Phi = \int d^4x \int_0^L dy \left\{ \Phi^\dagger (\partial_M \partial^M - M^2) \Phi - \frac{\lambda}{2} (\Phi^\dagger \Phi)^2 \right\}. \quad (94)$$

Here we introduce the 5D gauge bosons of  $G_M, W_M, B_M$ , which are 5D  $SU(3)_C, SU(2)_W, U(1)_Y$  ones, respectively.  $D_M$  means the covariant derivative for the corresponding gauge bosons. The 5D fermions in Eq. (28) are also gauged for reproducing the SM interactions.  $D_M$  and the action for the 5D gauge bosons take the same form with those in the mUED and we do not write down them since the detailed information is not important in the following discussion. The BCs for  $G_M, W_M, B_M$  are chosen as

$$\partial_y G_\mu|_{y=0} = \partial_y G_\mu|_{y=L} = 0, \quad (95)$$

$$G_y|_{y=0} = G_y|_{y=L} = 0, \quad (96)$$

where we only illustrate the gluon case. We write down a schematic diagram for explaining the BCs for bosons in Fig. 10. The green, orange and purple circular spots represent the ordinary Neumann, Dirichlet and the generalized BCs in Eq. (66), respectively. Except the both end points

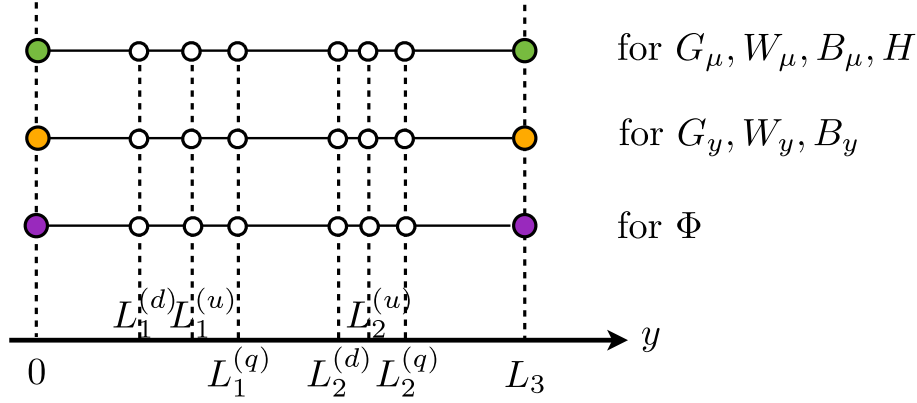


Figure 10: A schematic diagram for explaining the BCs for bosons. The green, orange and purple circular spots represent the ordinary Neumann, Dirichlet and the generalized BCs in Eq. (66), respectively. Except the both end points of the total system, we put the continuous condition discussed in Eqs. (24) and (25).

of the total system, we put the continuous condition discussed in Eqs. (24) and (25). Each 4D vector part has a zero mode, whose mode function is a constant. By putting the condition of  $M'^2 > 0$ , the  $SU(2)_W \times U(1)_Y$  gauge symmetry is spontaneously broken through the usual Higgs mechanism and the SM situation is duplicated at the sectors of  $G_M, W_M, B_M, H$ . Here we should assign the  $U(1)_Y$  charge of the Higgs singlet  $\Phi$  as zero to make the situation that  $\Phi$  do not couple to any gauge bosons. Accordingly, the problem in gauge universality never occurs in the refined setup.

What we should concern next is the structure of 5D Yukawa interactions. When we adopt the forms in the SM (or the mUED), the large mass hierarchy cannot be created since the profile of  $\langle H \rangle$  is constant. To simplify the situation, we introduce the following discrete symmetry

$$H \rightarrow -H, \quad \Phi \rightarrow -\Phi \quad (97)$$

to prohibit the terms of  $\bar{Q}(i\sigma_2 H^*)\mathcal{U}, \bar{Q}H\mathcal{D}, \Phi\bar{Q}Q, \Phi\bar{\mathcal{U}}\mathcal{U}, \Phi\bar{\mathcal{D}}\mathcal{D}$  with the Pauli matrix  $\sigma_2$ . The desirable 4D Yukawa structure is generated by introducing the following terms

$$S_Y = \int d^4x \int_0^L dy \left\{ \Phi \left[ -\mathcal{Y}^{(u)} \bar{Q}(i\sigma_2 H^*)\mathcal{U} - \mathcal{Y}^{(d)} \bar{Q}H\mathcal{D} + \text{h.c.} \right] \right\}, \quad (98)$$

where those operators are higher-dimensional compared to the previous five operators and allowed under the discrete symmetry in Eq. (97). We mention the coefficients  $\mathcal{Y}^{(u)}, \mathcal{Y}^{(d)}$  have mass dimension  $-2$ . After the ElectroWeak Symmetry Breaking (EWSB) occurs with nonvanishing  $\langle H \rangle$  and  $\langle \Phi \rangle$ , 4D effective Lagrangian which we assume in Eq. (28) is realized without any serious problem conflicting with the nature of the SM.

Here we discuss some related issues. Whether 5D gauge invariance is conserved or not is one of important criterion for judging validity of BCs. When we break gauge symmetry by BCs, the issue of possible unitary violation due to longitudinal components of massive gauge bosons should be considered [62–64]. We, however, mention that in the cases of the Dirichlet BC for the fermions at mid and end points and the generalized Higgs BC at end points, 5D gauge invariance is intact.

In the above analysis, we neglect the contribution to the total scalar potential of the doublet-

singlet mixing term with a coefficient  $C$

$$S_{\text{mixing}} = \int d^4x \int_0^L dy \left\{ -C \Phi^\dagger \Phi H^\dagger H \right\}, \quad (99)$$

where the discrete symmetry in Eq. (97) cannot ban this form. After considering this part, the profiles of  $\Phi$  and  $H$  are deformed and the problem in gauge universality is revived. Therefore we should choose a sufficiently small coefficient  $C$  to avoid this obstacle. The detailed discussion is done in Appendix A.

#### 4.4 Detailed numerical calculations for justifying the model with Higgs doublet and singlet

Based on the previous discussions, we reexamine the issue for validness of our model including the Higgs doublet and scalar singlet with numerical calculations. At first, we reconsider the approximation in Eq. (81). As we have discussed before, the cn function is almost equivalent to the cosh function in the limit of  $k \simeq 1$ , and then we obtain the form

$$\langle \Phi(y) \rangle \simeq \nu \cosh \left[ \sqrt{\frac{\lambda}{2}} \mu (y - y_0) \right] = \frac{\nu}{2} \left\{ e^{\sqrt{\frac{\lambda}{2}} \mu (y - y_0)} + e^{-\sqrt{\frac{\lambda}{2}} \mu (y - y_0)} \right\} \quad (\text{with } k \simeq 1). \quad (100)$$

If the condition  $\sqrt{\frac{\lambda}{2}} \mu (y - y_0) \gtrsim 1$  is fulfilled, the second term on the right-hand-side of Eq. (100) can be neglected within about 10% error ( $e^{-2} \simeq 0.135$ ). Therefore we get the outcome of

$$\langle \Phi(y) \rangle \simeq \frac{\nu}{2} e^{\sqrt{\frac{\lambda}{2}} \mu (y - y_0)} \quad \left( \text{with } k \simeq 1 \text{ and } \sqrt{\frac{\lambda}{2}} \mu (y - y_0) \gtrsim 1 \right). \quad (101)$$

Here we consider the situation of  $k \simeq 1$  more concretely. As we show in Eq. (73), the parameter  $k$  is composed by some input parameters for the solution and  $k \simeq 1$  is equal to the condition

$$X = \frac{4\lambda |Q|}{M^4} \simeq 0. \quad (102)$$

It is obvious that for matching up to this condition, the smaller (greater) value of  $\lambda$  and/or  $|Q|$  ( $M$ ) is preferred. But the extremal choices of  $\lambda = 0$ ,  $|Q| = 0$ ,  $M = \infty$  turn into disorder and unnaturalness. We rewrite the approximated form in Eq. (101) with input parameters by considering the shapes of  $\mu, \nu$  in Eqs. (70) and (71), which are roughly under the situation  $k \simeq 1$

$$\mu \simeq \sqrt{\frac{2}{\lambda}} M, \quad \nu \simeq \frac{\sqrt{2|Q|}}{M}, \quad (103)$$

with the zeroth (first) order approximation in  $X$  for  $\mu$  ( $\nu$ ). When we evaluate  $\nu$  up to  $X$ 's zeroth order, the value of  $\nu$  goes to zero and this is meaningless. By use of the results, we can rewrite the equation in (101) as

$$\langle \Phi(y) \rangle \simeq \sqrt{\frac{|Q|}{2}} \frac{1}{M} e^{-My_0} \cdot e^{My} \quad (\text{with } k \simeq 1 \text{ and } M(y - y_0) \gtrsim 1). \quad (104)$$



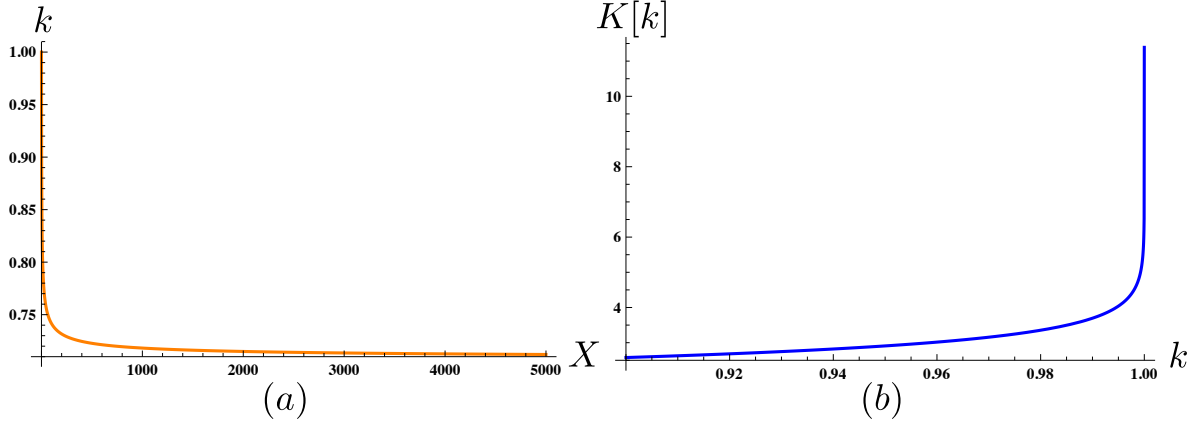


Figure 11: (a) the value of  $k$  in the function of  $X$  in the range of  $0 \leq X \leq 5000$ . (b) the value of the complete elliptic integral of the first kind  $K[k]$  in the range of  $0.9 \leq k \leq 1$ .

The correspondence of Eq. (104) to the assumed warped VEV in Eq. (31) is as follows:

$$\mathcal{A} = \sqrt{\frac{|Q|}{2}} \frac{1}{M} e^{M(L-y_0)}, \quad \alpha = M. \quad (105)$$

Then we notice that the shape of the approximated profile in Eq. (104) is mainly determined by  $M, y_0$ , and that  $\lambda$  does not appear up to the approximation.

In what follows, we discuss the validness of the above approximation and the deviation from it when we consider the exact form in Eq. (75). At first, we define the dimensionless parameters with tilde  $\tilde{\phantom{x}}$  in the basis of the massive parameter of the total length of the system  $L (= L_3)$ , *e.g.*,

$$M = \tilde{M}L^{-1}, \quad L_i^{(q)} = \tilde{L}_i^{(q)}L, \quad (106)$$

where part of the dimensionless parameters is already calculated in Eq. (58). The significant point is the bulk mass of the Higgs singlet is already almost fixed because of Eqs. (58), (104) and (105) as

$$M \simeq 8.67L^{-1}, \quad (107)$$

and then we should search for a region of the parameters related to the singlet under the constraint.

In our configuration, the modulus parameter of the Jacobi's elliptic function  $\text{cn}$  is determined as a function of  $X = \frac{4\lambda|Q|}{M^4}$  as in Eq. (73) and the relation between them is shown in Fig. 11, where we understand that we have to take very small  $X$  for obtaining  $k = 1$ . We also refer to the complete elliptic integral of the first kind  $K[k]$ , which is the function of the elliptic modulus  $k$  and whose value is equal to the quarter period of the Jacobi's elliptic function  $\text{cn}(y, k)$  in Fig. 11. This plot suggests that if we take the infinite period, whose case corresponds to  $1/\cosh(y, k)$ , we tune the value of  $k$  very close to one.

Positions of divergent points of  $1/\text{cn}(x, k)$ , which correspond to zero points of  $\text{cn}(x, k)$ , give us another important suggestion. The  $1/\text{cn}(x, k)$  function gets divergent with a period of  $2K[k]$  and the range of  $[0, L]$  should not contain any such point. In the exact form of the VEV  $\langle \Phi(y) \rangle$  in

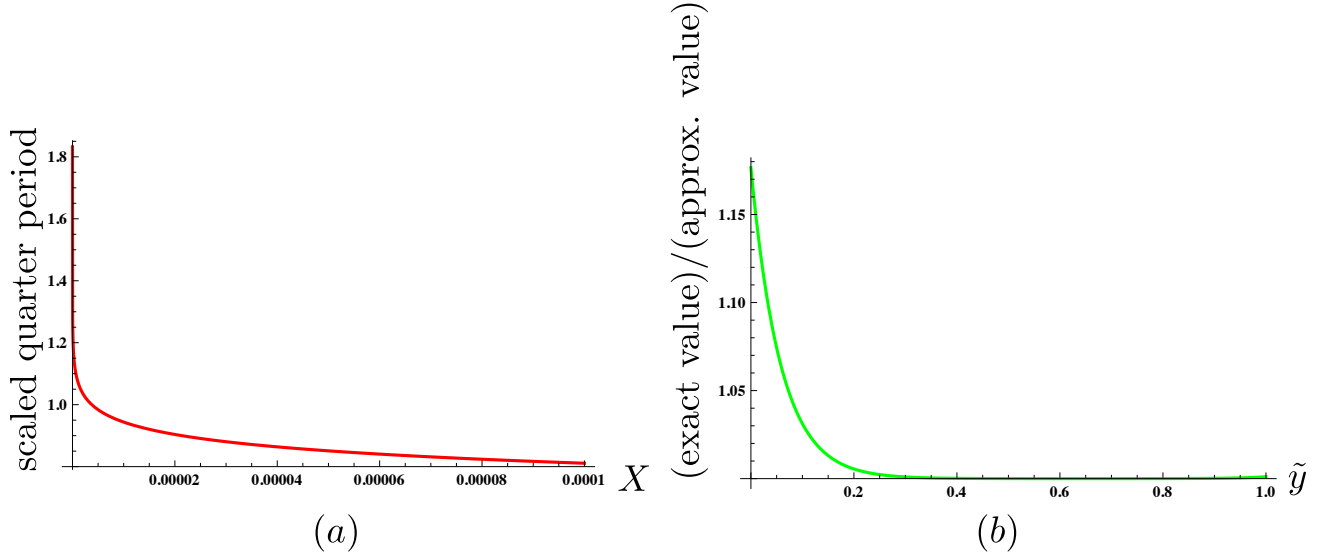


Figure 12: (a) the value of the scaled quarter period of the exact VEV in the function of  $X$  in the range of  $0 \leq X \leq 0.0001$ . (b) the value of the ratio, which is defined as the exact VEV form over its approximated form in Eq. (104).

Eq. (75), the position  $y_d$  with divergence is evaluated as

$$\tilde{y}_d = \tilde{y}_0 + \frac{1}{\tilde{M}(1+X)^{1/4}} K \left[ \sqrt{\frac{1}{2} \left( 1 + \frac{1}{\sqrt{1+X}} \right)} \right] \quad \left( \text{mod } \frac{2}{\tilde{M}(1+X)^{1/4}} K \left[ \sqrt{\frac{1}{2} \left( 1 + \frac{1}{\sqrt{1+X}} \right)} \right] \right) \quad (108)$$

with  $X = \tilde{X} = \frac{4\tilde{\lambda}|\tilde{Q}|}{\tilde{M}^4}$ . The second term of the right side in Eq. (108) means the quarter period of  $\langle \Phi(y) \rangle$  in the coordinate  $\tilde{y}$ . Considering the profile in Fig. 8, in the scaled coordinate  $\tilde{y}$  the position of  $\tilde{y}_d$  is preferred at one plus a few positive values. When we consider the property of the scaled quarter period in Fig. 12, as we have discussed before, we need to make the value of  $X$  approach to zero (but not exact zero) for  $\mathcal{O}(1)$  scaled period. In addition, we have to take account of the condition on  $y_0$  in Eq. (104), which is interpreted in the scaled coordinate  $\tilde{y}$  as

$$\tilde{M}(\tilde{y} - \tilde{y}_0) \gtrsim 1 \rightarrow 8.67(\tilde{y} - \tilde{y}_0) \gtrsim 1 \quad \text{in the range of } 0 \leq \tilde{y} \leq 1, \quad (109)$$

with the value of dimensionless  $\tilde{M}$  in Eq. (107). Here we observe that the case of positive  $\tilde{y}_0$  is problematic (at least) around  $\tilde{y} = 0$ . Based on all the knowledge which we have obtained, we can find a set of parameters

$$\tilde{M} = 8.67, \quad \tilde{y}_0 = -0.1, \quad \tilde{\lambda} = 0.001, \quad |\tilde{Q}| = 0.001. \quad (110)$$

The validity of this choice is checked in Fig. 12 to calculate the ratio, which is defined as the exact VEV form over its approximated form in Eq. (104), and the difference is estimated as about fifteen percent at most.

In the following, we check whether the EWSB occurs or not in our configuration. The prescription is written in the Section 4.2 and the two input parameters  $L_{\pm}$  can be inversely calculated from the profile of the exact VEV through Eq. (76) as

$$\frac{1}{\tilde{L}_+} = -6.07, \quad \frac{1}{\tilde{L}_-} = 8.69 \quad (111)$$

and the value of  $\tilde{L}_{\max}$  in Eq. (78) is simultaneously fixed  $1/\tilde{L}_{\max} = 8.69$  as the scaled values based on  $L$ . Agreeing with the previous naive discussion at the end of Section 4.2, the condition

$$M^2 < \frac{1}{L_{\max}^2} \quad (112)$$

is fulfilled and then the EWSB is realized in our configuration for real. Here we comment on the two things. One is that the parameter  $\lambda$  always appears in the cn function as the combination of  $|Q|\lambda$  and  $\lambda$  in itself only affects on the overall normalization. This means that we can take more greater value in  $\lambda$  with more smaller  $|Q|$ . The other is that the smallness of  $y_0$  and  $|Q|$  is not unnatural thing, because they are resultant values derived from the two input parameters  $L_{\pm}$ , whose dimensionless values are within  $\mathcal{O}(10)$ .

Owing to the above discussion, we are able to calculate Yukawa mass matrix elements in our model with the “elliptic VEV”  $\langle \Phi(y) \rangle$ . We take care of the following two facts:

- We use the exact form of the VEV in Eq. (75) instead of the assumed warped form in Eq. (31) with the parameters in Eqs. (110) and/or (111).
- Because the Yukawa structure is introduced as the higher-dimensional operators in Eq. (98), the replacement is required

$$Y^{(u)} \rightarrow \mathcal{Y}^{(u)} \frac{v}{\sqrt{2}}, \quad Y^{(d)} \rightarrow \mathcal{Y}^{(d)} \frac{v}{\sqrt{2}}. \quad (113)$$

The diagonalized Yukawa mass matrices take the forms of

$$\mathcal{M}^{(u)}|_{\text{diagonal}} = \text{diag}(2.47 \text{ MeV}, 1.18 \text{ GeV}, 174 \text{ GeV}), \quad (114)$$

$$\mathcal{M}^{(d)}|_{\text{diagonal}} = \text{diag}(3.94 \text{ MeV}, 110 \text{ MeV}, 4.19 \text{ GeV}), \quad (115)$$

and the CKM matrix is given as

$$|V_{\text{CKM}}| = \begin{bmatrix} 0.977 & 0.214 & 0.00448 \\ 0.213 & 0.976 & 0.0475 \\ 0.0145 & 0.0454 & 0.999 \end{bmatrix}, \quad (116)$$

where we adopt the values in Eq. (58) for the 9 lengths ( $L_1^{(q)}, L_2^{(q)}, L_3^{(q)}, L_1^{(u)}, L_2^{(u)}, L_3^{(u)}, L_1^{(d)}, L_2^{(d)}, L_3^{(d)}$ ) and the 3 fermion bulk masses ( $M_Q, M_U, M_D$ ). We can find only a small difference between the results and the previous results based on the assumed warped VEV.

In contrast to the foregoing analysis, the Higgs dynamics is well described and the dimensionless coefficient part of  $\langle \Phi(y) \rangle$ , which is related to  $\tilde{\mathcal{A}}$  in the assumed warped VEV, is calculable and the values of  $\tilde{\mathcal{Y}}^{(u)}, \tilde{\mathcal{Y}}^{(d)}$  are as follows:

$$\tilde{\mathcal{Y}}^{(u)} = 0.0442, \quad \tilde{\mathcal{Y}}^{(d)} = 0.00369. \quad (117)$$

Here we mention that when we consider the situation where all the objects are localized, the effective length of each object is considered to be smaller than the total length  $L$ . If we take the effective length for overlap integrals showing down quarks as about  $L/3$ , which is the length of the integral for  $m_{11}^{(d)}$ , the unnaturalsness in  $\tilde{\mathcal{Y}}^{(d)}$  is somewhat ameliorated as follows:

$$\tilde{\mathcal{Y}}^{(d)} \sim 0.00369 \cdot (3)^2 = 0.0332. \quad (118)$$

The insertion of the relatively-large massive value  $v = 246 \text{ GeV}$ , compared to the quark masses except top quark’s one, to the 5D Yukawa structure in Eq (113) is a cause of the smallness of  $\tilde{\mathcal{Y}}^{(u)}$  and  $\tilde{\mathcal{Y}}^{(d)}$ . We do not go for more detailed discussion since we cannot avoid some ambiguities.

## 5 Summary and discussions

We have presented a review on some properties of 5D fermion and vector fields in multi-interval system, where each interval is connected to the others through point interactions. By choosing BCs at the positions of point interactions suitably, the profiles of fermion zero modes get to be three-fold degenerated, localized, and mixed, which means all of the Yukawa structure in the SM can be realized. Combined with the  $y$ -position-dependent Higgs VEV with exponential warped form, the quark mass hierarchy and the structure of the CKM matrix are explained simultaneously almost only via geometry of extra dimension. One way to generate the warped VEV without gauge universality violation is to introduce both of the Higgs doublet with the ordinary Neumann BCs and the scalar singlet with the generalized BCs, which are coupled in higher-dimensional Yukawa terms. The ordinary Yukawa terms are prohibited by adding a discrete symmetry. The exact form of the scalar singlet VEV is written by the Jacobi's elliptic function and we have found that it becomes close to the exponential function in a region of parameters with almost  $\mathcal{O}(10)$  input parameters. To avoid violation in gauge universality, we should assume that the magnitude of the coefficient of the doublet-singlet mixing term in Eq. (99) is sufficiently small.

Here we estimate the effect from KK mixing shortly. In our system, translational invariance along  $y$  is highly violated because of the existence of the point interactions and moreover KK-parity cannot be defined in behalf of lack of reflection symmetry. Consequently, the zero modes and KK modes of the fermions are mixed at the tree level and this affect the value of the mass eigenstates and the elements of the CKM matrix. Here we would like to consider the following form

$$- \left[ \bar{t}^{(0)}, \bar{T}^{(1)}, \bar{t}^{(1)} \right]_L \begin{bmatrix} m_t & 0 & m_t \\ m_t & M_{KK} & m_t \\ 0 & m_t & M_{KK} \end{bmatrix} \begin{bmatrix} t^{(0)} \\ T^{(1)} \\ t^{(1)} \end{bmatrix}_R + \text{h.c.}, \quad (119)$$

where  $m_t, M_{KK}, t^{(0)}, T^{(1)}, t^{(1)}$  are the top quark mass, KK scale, top zero mode, first top KK state of  $SU(2)_W$  doublet, that of  $SU(2)_W$  singlet, respectively. In the following, we only consider the mixing in the top quark sector because mixings in the other five flavors are negligible because of smallness of their Yukawa couplings. In reality some deviation factors from the assumed ordinary UED-like form probably emerge in front of each matrix component originated from difference in overlap integrals and mixings between a zero mode and/or between zero modes and KK states of more than first level are also derived. But we ignore these issues for simplicity.

The deviation ratio in the observed top mass, which is defined as the mass eigenvalues over the reference value 172 GeV is calculated and the results is represented in Fig. 13. Then we conclude that we can ignore the level-mixing effect when the KK scale, which is defined as  $\pi/L$  in the ordinary UED context, is greater than 300 GeV up to accepting our naive assumptions. More detail analysis is out of the scope of this paper and we will discuss this issue in a future study. It is noted that in a “decoupling” case with a huge  $M_{KK}$ , we can always neglect the level mixing effect even if this possibility is not so interesting in collider physics point of view.

The work done in this paper is considered as a first step for constructing a phenomenological model which explains the number of fermion generation, fermion mass hierarchies, and the structure of fermion mixing matrices simultaneously mainly based on geometry of an extra dimension. But lots of issues to be studied remain.

The first issue is whether our mechanism works well in the lepton sector. As widely known, two mixing angles of neutrinos are large, and this suggests that the components of neutrino mass matrix are probably the same order of magnitude in contrast to the quark one. In addition, the expected neutrino masses are up to (sub-)eV order, where we find at least six orders of magnitude

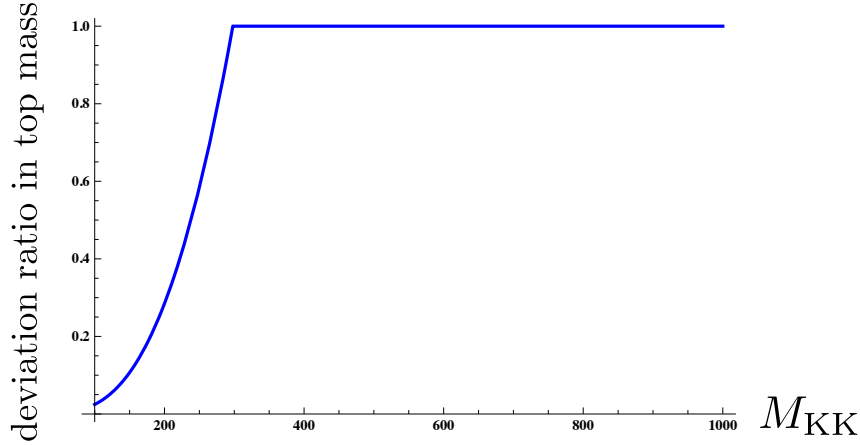


Figure 13: The deviation ratio in the observed top mass, which is defined as the mass eigenvalues over the reference value 172 GeV.

smaller than the value of the lightest charged lepton (electron). These differences are nontrivial and we will search for a configuration where the properties of the quarks and leptons are derived simultaneously via geometry. The second related issue is on the phase of CP violation in the CKM matrix. The existence of this phase with nonzero value has been established by B physics experiments, but within our present mechanism such a phase never occurs since all the zero mode functions are real. One considerable direction to overcome this problem is to introduce a complex phase through twisted boundary conditions.

Some away from phenomenological issue, the Higgs with the generalized boundary conditions has a rich theoretical structure and there many topics wait for being unveiled. The phase structure of the scalar singlet is explored in Ref. [60] but for non-singlet scalars some limited studies have been done. In non-Abelian gauge theory the boundary conditions can mix the gauge indices and possibilities are enlarged. Accordingly its phase structure gets to be much richer. Another interesting issue is the structure of quantum fluctuation around the position-dependent elliptic VEV of the singlet scalar. Even in the case of the zero mode, the properties are highly nontrivial but this issue is mandatory when we discuss the signature of the scalar singlet at colliders. Moduli stabilization via Casimir energy is also an important topic for ensuring the stability of the system with the nontrivial VEV structure.<sup>6</sup>

The physics in the system with point interactions and/or  $y$ -position-dependent scalar VEV just only starts to be dug out and we can find a lot of fascinating themes in both phenomenological and theoretical points of view.

## Acknowledgments

The authors at first appreciate S.Ohya for giving us many fruitful comments and reading our manuscript carefully. The authors would like to thank T.Kugo, N.Maru, K.-y.Oda, J.Sato, Y.Shimizu, R.Takahashi, M.Yamanaka and T.Yamashita for valuable discussions. K.N. is partially supported by funding available from the Department of Atomic Energy, Government of India for the Regional Centre for Accelerator-based Particle Physics (RECAPP), Harish-Chandra Research Institute. This work is supported in part by a Grant-in-Aid for Scientific Research (No.22540281 and No.20540274 (M.S.)) from the Japanese Ministry of Education, Science, Sports and Culture.

<sup>6</sup> We can find some related works in Refs. [65–67].

## Appendix

### A Estimating the orders of magnitude of doublet-singlet scalars mixing effect

In this Appendix, we consider the minimization problem of the scalar potential of the doublet  $H$  and singlet  $\Phi$  scalars with the doublet-singlet mixing term in Eq. (99). In this analysis, we assume that the VEV of the singlet  $\Phi$  takes the effective form  $\langle\phi(y)\rangle$  in Eq. (31) and we concentrate on the part of

$$\int d^4x \int_0^L dy \left\{ H^\dagger (\partial_y)^2 H + M'^2 H^\dagger H - \frac{\lambda'}{2} (H^\dagger H)^2 - C \Phi^\dagger \Phi H^\dagger H \right\}. \quad (120)$$

After the replacement

$$H \rightarrow \begin{pmatrix} 0 \\ \frac{\langle h(y) \rangle}{\sqrt{2}} \end{pmatrix}, \quad \Phi \rightarrow \langle \phi(y) \rangle, \quad (121)$$

we can identify the functional form  $\mathcal{E}'[\langle h \rangle]$  which we should minimize as follows:

$$\mathcal{E}'[\langle h \rangle] = \int_0^L dy \left\{ (\partial_y \langle h \rangle)^2 - M'^2 \langle h \rangle^2 + \frac{\lambda'}{4} \langle h \rangle^4 + C \langle \phi \rangle^2 \langle h \rangle^2 \right\}. \quad (122)$$

Due to the Neumann BCs in Eq. (92), the form of the (position-dependent) VEV  $\langle h(y) \rangle$  is fixed as

$$\langle h(y) \rangle = \sqrt{\frac{2}{\lambda'}} M' + \beta_0 + \sum_{n=1}^{\infty} \beta_n \cos\left(\frac{\pi n}{L} y\right), \quad (123)$$

with the coefficients  $\beta_0, \beta_n$ . Here the first term of the right-handed side of Eq. (123) corresponds to the solution with  $C = 0$ , whose value is equal to  $v/\sqrt{2L}$  with  $v = 246$  GeV, and the remaining two terms show the deformation from it in the case of  $C \neq 0$ . Under the assumption that the value of  $C$  is small, the potential is minimized with the forms of the coefficients

$$\beta_0 = -\frac{\sqrt{\frac{2}{\lambda'}} C}{2M'L} \frac{\mathcal{A}^2}{2\alpha} (1 - e^{-2\alpha L}), \quad (124)$$

$$\beta_n = -\frac{2\sqrt{\frac{2}{\lambda'}} M' C}{L \left[ 2M'^2 + \left(\frac{\pi n}{L}\right)^2 \right]} \frac{\mathcal{A}^2}{2} \frac{4\alpha}{4\alpha^2 + \left(\frac{\pi n}{L}\right)^2} ((-1)^n - e^{-2\alpha L}), \quad (125)$$

within the second order of  $C$ .

After we consider the suitable order estimation

$$\lambda' \sim L, \quad M' \sim v, \quad \mathcal{A}\sqrt{L} \sim v, \quad L^{-1} \sim M_{\text{KK}}, \quad \alpha L \sim \mathcal{O}(1), \quad (126)$$

where  $M_{\text{KK}}$  is a typical mass scale of the KK states, we can conclude that the orders of magnitude of the deviation from  $C = 0$  as

$$\left| \frac{\beta_0}{\sqrt{\frac{2}{\lambda'}} M'} \right| \sim \frac{\tilde{C}}{\tilde{\alpha}}, \quad (127)$$

$$\left| \frac{\beta_n}{\sqrt{\frac{2}{\lambda'}} M'} \right| \sim \frac{\tilde{\alpha}}{n^2 (n^2 + \tilde{\alpha}^2)} \left( \frac{v}{M_{\text{KK}}} \right)^2 \tilde{C}, \quad (128)$$

with the dimensionless values  $\alpha = \tilde{\alpha} L^{-1}$ ,  $C = \tilde{C} L$ . The results tell us that the value of  $\beta_n$  is suppressed by the KK index  $n$  and  $M_{\text{KK}}$ , but on the contrary, that of  $\beta_0$  is not suppressed because of  $\tilde{\alpha} = \mathcal{O}(1)$  in Eqs. (58) and (126) although  $\beta_0$  does not affect our conclusions since it merely shifts the constant expectation value of  $H$ . On the other hand, nonzero values of  $\beta_n$  could cause a problem of gauge universality, so that  $\tilde{C}$  ( $M_{\text{KK}}$ ) should be sufficiently small (large) in our model.

## References

- [1] **ATLAS Collaboration** Collaboration, G. Aad *et al.*, “Observation of a new particle in the search for the Standard Model Higgs boson with the ATLAS detector at the LHC,” *Phys.Lett.* **B716** (2012) 1–29, [arXiv:1207.7214 \[hep-ex\]](#).
- [2] **CMS Collaboration** Collaboration, S. Chatrchyan *et al.*, “Observation of a new boson at a mass of 125 GeV with the CMS experiment at the LHC,” *Phys.Lett.* **B716** (2012) 30–61, [arXiv:1207.7235 \[hep-ex\]](#).
- [3] N. Arkani-Hamed, S. Dimopoulos, and G. R. Dvali, “The Hierarchy problem and new dimensions at a millimeter,” *Phys.Lett.* **B429** (1998) 263–272, [arXiv:hep-ph/9803315 \[hep-ph\]](#).
- [4] L. Randall and R. Sundrum, “A Large mass hierarchy from a small extra dimension,” *Phys.Rev.Lett.* **83** (1999) 3370–3373, [arXiv:hep-ph/9905221 \[hep-ph\]](#).
- [5] Y. Hosotani, “Dynamical Mass Generation by Compact Extra Dimensions,” *Phys.Lett.* **B126** (1983) 309.
- [6] Y. Hosotani, “Dynamics of Nonintegrable Phases and Gauge Symmetry Breaking,” *Annals Phys.* **190** (1989) 233.
- [7] H. Hatanaka, T. Inami, and C. S. Lim, “The Gauge hierarchy problem and higher dimensional gauge theories,” *Mod.Phys.Lett.* **A13** (1998) 2601–2612, [arXiv:hep-th/9805067 \[hep-th\]](#).
- [8] Y. Kawamura, “Gauge symmetry breaking from extra space  $S^1/Z_2$ ,” *Prog.Theor.Phys.* **103** (2000) 613–619, [arXiv:hep-ph/9902423 \[hep-ph\]](#).
- [9] Y. Kawamura, “Triplet doublet splitting, proton stability and extra dimension,” *Prog.Theor.Phys.* **105** (2001) 999–1006, [arXiv:hep-ph/0012125 \[hep-ph\]](#).

- [10] A. Hebecker and J. March-Russell, “The structure of GUT breaking by orbifolding,” *Nucl.Phys.* **B625** (2002) 128–150, [arXiv:hep-ph/0107039](#) [hep-ph].
- [11] G. Dvali and A. Y. Smirnov, “Probing large extra dimensions with neutrinos,” *Nucl.Phys.* **B563** (1999) 63–81, [arXiv:hep-ph/9904211](#) [hep-ph].
- [12] R. Mohapatra, S. Nandi, and A. Perez-Lorenzana, “Neutrino masses and oscillations in models with large extra dimensions,” *Phys.Lett.* **B466** (1999) 115–121, [arXiv:hep-ph/9907520](#) [hep-ph].
- [13] K. Yoshioka, “On fermion mass hierarchy with extra dimensions,” *Mod.Phys.Lett.* **A15** (2000) 29–40, [arXiv:hep-ph/9904433](#) [hep-ph].
- [14] N. Arkani-Hamed, S. Dimopoulos, G. R. Dvali, and J. March-Russell, “Neutrino masses from large extra dimensions,” *Phys.Rev.* **D65** (2002) 024032, [arXiv:hep-ph/9811448](#) [hep-ph].
- [15] Y. Grossman and M. Neubert, “Neutrino masses and mixings in nonfactorizable geometry,” *Phys.Lett.* **B474** (2000) 361–371, [arXiv:hep-ph/9912408](#) [hep-ph].
- [16] T. Gherghetta and A. Pomarol, “Bulk fields and supersymmetry in a slice of AdS,” *Nucl.Phys.* **B586** (2000) 141–162, [arXiv:hep-ph/0003129](#) [hep-ph].
- [17] S. J. Huber and Q. Shafi, “Fermion masses, mixings and proton decay in a Randall-Sundrum model,” *Phys.Lett.* **B498** (2001) 256–262, [arXiv:hep-ph/0010195](#) [hep-ph].
- [18] M. V. Libanov and S. V. Troitsky, “Three fermionic generations on a topological defect in extra dimensions,” *Nucl.Phys.* **B599** (2001) 319–333, [arXiv:hep-ph/0011095](#) [hep-ph].
- [19] J. M. Frere, M. V. Libanov, and S. V. Troitsky, “Three generations on a local vortex in extra dimensions,” *Phys.Lett.* **B512** (2001) 169–173, [arXiv:hep-ph/0012306](#) [hep-ph].
- [20] J. M. Frere, M. V. Libanov, and S. V. Troitsky, “Neutrino masses with a single generation in the bulk,” *JHEP* **0111** (2001) 025, [arXiv:hep-ph/0110045](#) [hep-ph].
- [21] H. B. Nielsen and P. Olesen, “Vortex Line Models for Dual Strings,” *Nucl.Phys.* **B61** (1973) 45–61.
- [22] A. Neronov, “Fermion masses and quantum numbers from extra dimensions,” *Phys.Rev.* **D65** (2002) 044004, [arXiv:gr-qc/0106092](#) [gr-qc].
- [23] M. Gogberashvili, P. Midodashvili, and D. Singleton, “Fermion Generations from ‘Apple-Shaped’ Extra Dimensions,” *JHEP* **0708** (2007) 033, [arXiv:0706.0676](#) [hep-th].
- [24] D. B. Kaplan and S. Sun, “Spacetime as a topological insulator: Mechanism for the origin of the fermion generations,” *Phys.Rev.Lett.* **108** (2012) 181807, [arXiv:1112.0302](#) [hep-ph].
- [25] N. Arkani-Hamed and M. Schmaltz, “Hierarchies without symmetries from extra dimensions,” *Phys.Rev.* **D61** (2000) 033005, [arXiv:hep-ph/9903417](#) [hep-ph].
- [26] V. A. Rubakov and M. E. Shaposhnikov, “Do We Live Inside a Domain Wall?,” *Phys.Lett.* **B125** (1983) 136–138.



- [27] K. Akama, “An Early Proposal of ‘Brane World’,” *Lect.Notes Phys.* **176** (1982) 267–271, [arXiv:hep-th/0001113](#) [hep-th].
- [28] G. R. Dvali and M. A. Shifman, “Families as neighbors in extra dimension,” *Phys.Lett.* **B475** (2000) 295–302, [arXiv:hep-ph/0001072](#) [hep-ph].
- [29] D. E. Kaplan and T. M. P. Tait, “New tools for fermion masses from extra dimensions,” *JHEP* **0111** (2001) 051, [arXiv:hep-ph/0110126](#) [hep-ph].
- [30] H. Hatanaka, M. Sakamoto, M. Tachibana, and K. Takenaga, “Many brane extension of the Randall-Sundrum solution,” *Prog.Theor.Phys.* **102** (1999) 1213–1218, [arXiv:hep-th/9909076](#) [hep-th].
- [31] T. Nagasawa, M. Sakamoto, and K. Takenaga, “Supersymmetry in quantum mechanics with point interactions,” *Phys.Lett.* **B562** (2003) 358–364, [arXiv:hep-th/0212192](#) [hep-th].
- [32] T. Nagasawa, M. Sakamoto, and K. Takenaga, “Supersymmetry and discrete transformations on  $S^1$  with point singularities,” *Phys.Lett.* **B583** (2004) 357–363, [arXiv:hep-th/0311043](#) [hep-th].
- [33] T. Nagasawa, M. Sakamoto, and K. Takenaga, “Extended supersymmetry and its reduction on a circle with point singularities,” *J.Phys.* **A38** (2005) 8053–8082, [arXiv:hep-th/0505132](#) [hep-th].
- [34] T. Appelquist, H.-C. Cheng, and B. A. Dobrescu, “Bounds on universal extra dimensions,” *Phys. Rev.* **D64** (2001) 035002, [arXiv:hep-ph/0012100](#).
- [35] G. Servant and T. M. P. Tait, “Is the lightest Kaluza-Klein particle a viable dark matter candidate?,” *Nucl.Phys.* **B650** (2003) 391–419, [arXiv:hep-ph/0206071](#) [hep-ph].
- [36] T. Flacke, A. Menon, and D. J. Phalen, “Non-minimal universal extra dimensions,” *Phys.Rev.* **D79** (2009) 056009, [arXiv:0811.1598](#) [hep-ph].
- [37] A. Datta, U. K. Dey, A. Shaw, and A. Raychaudhuri, “Universal Extra-Dimensional models with boundary localized kinetic terms: Probing at the LHC,” [arXiv:1205.4334](#) [hep-ph].
- [38] A. Datta, K. Nishiwaki, and S. Niyogi, “Non-minimal Universal Extra Dimensions: The strongly interacting sector at the Large Hadron Collider,” [arXiv:1206.3987](#) [hep-ph].
- [39] T. Flacke, A. Menon, and Z. Sullivan, “Constraints on UED from W’ searches,” [arXiv:1207.4472](#) [hep-ph].
- [40] G. Belanger, M. Kakizaki, and A. Pukhov, “Dark matter in UED: The Role of the second KK level,” *JCAP* **1102** (2011) 009, [arXiv:1012.2577](#) [hep-ph].
- [41] K. Nishiwaki, “Higgs production and decay processes via loop diagrams in various 6D Universal Extra Dimension Models at LHC,” *JHEP* **1205** (2012) 111, [arXiv:1101.0649](#) [hep-ph].
- [42] K. Nishiwaki, K.-y. Oda, N. Okuda, and R. Watanabe, “A bound on Universal Extra Dimension Models from up to  $2\text{fb}^{-1}$  of LHC Data at 7TeV,” *Phys.Lett.* **B707** (2012) 506–511, [arXiv:1108.1764](#) [hep-ph].

- [43] G. Belanger, A. Belyaev, M. Brown, M. Kakizaki, and A. Pukhov, “Higgs Phenomenology of Minimal Universal Extra Dimensions,” *EPJ Web Conf.* **28** (2012) 12070, [arXiv:1201.5582 \[hep-ph\]](#).
- [44] T. Kakuda, K. Nishiwaki, K.-y. Oda, N. Okuda, and R. Watanabe, “Higgs at ILC in Universal Extra Dimensions in Light of Recent LHC Data,” [arXiv:1202.6231 \[hep-ph\]](#).
- [45] G. Belanger, A. Belyaev, M. Brown, M. Kakizaki, and A. Pukhov, “Testing Minimal Universal Extra Dimensions Using Higgs Boson Searches at the LHC,” [arXiv:1207.0798 \[hep-ph\]](#).
- [46] M. Sakamoto, M. Tachibana, and K. Takenaga, “Spontaneously broken translational invariance of compactified space,” *Phys.Lett.* **B457** (1999) 33–38, [arXiv:hep-th/9902069 \[hep-th\]](#).
- [47] M. Sakamoto, M. Tachibana, and K. Takenaga, “Spontaneous supersymmetry breaking from extra dimensions,” *Phys.Lett.* **B458** (1999) 231–236, [arXiv:hep-th/9902070 \[hep-th\]](#).
- [48] M. Sakamoto, M. Tachibana, and K. Takenaga, “A New mechanism of spontaneous SUSY breaking,” *Prog.Theor.Phys.* **104** (2000) 633–676, [arXiv:hep-th/9912229 \[hep-th\]](#).
- [49] K. Ohnishi and M. Sakamoto, “Novel phase structure of twisted  $O(N)$   $\phi^4$  model on  $M^{D-1} \otimes S^1$ ,” *Phys.Lett.* **B486** (2000) 179–185, [arXiv:hep-th/0005017 \[hep-th\]](#).
- [50] H. Hatanaka, S. Matsumoto, K. Ohnishi, and M. Sakamoto, “Vacuum structure of twisted scalar field theories on  $M^{D-1} \otimes S^1$ ,” *Phys.Rev.* **D63** (2001) 105003, [arXiv:hep-th/0010283 \[hep-th\]](#).
- [51] S. Matsumoto, M. Sakamoto, and S. Tanimura, “Spontaneous breaking of the rotational symmetry induced by monopoles in extra dimensions,” *Phys.Lett.* **B518** (2001) 163–170, [arXiv:hep-th/0105196 \[hep-th\]](#).
- [52] M. Sakamoto and S. Tanimura, “Spontaneous breaking of the C, P, and rotational symmetries by topological defects in extra two dimensions,” *Phys.Rev.* **D65** (2002) 065004, [arXiv:hep-th/0108208 \[hep-th\]](#).
- [53] M. Reed and B. Simon, *Methods of Modern Mathematical Physics: Fourier analysis, self-adjointness*. New York: Academic, 1975.
- [54] P. Šeba, “The generalized point interaction in one dimension,” *Czechoslovak Journal of Physics* **36** (1986) 667.
- [55] T. Cheon, T. Fulop, and I. Tsutsui, “Symmetry, duality and anholonomy of point interactions in one dimension,” *Annals Phys.* **294** (2001) 1–23, [arXiv:quant-ph/0008123 \[quant-ph\]](#).
- [56] T. Nagasawa, S. Ohya, K. Sakamoto, M. Sakamoto, and K. Sekiya, “Hierarchy of QM SUSYs on a Bounded Domain,” *J.Phys.* **A42** (2009) 265203, [arXiv:0812.4659 \[hep-th\]](#).
- [57] C. S. Lim, T. Nagasawa, M. Sakamoto, and H. Sonoda, “Supersymmetry in gauge theories with extra dimensions,” *Phys.Rev.* **D72** (2005) 064006, [arXiv:hep-th/0502022 \[hep-th\]](#).

- [58] C. S. Lim, T. Nagasawa, S. Ohya, K. Sakamoto, and M. Sakamoto, “Supersymmetry in 5d gravity,” *Phys.Rev.* **D77** (2008) 045020, [arXiv:0710.0170 \[hep-th\]](#).
- [59] C. S. Lim, T. Nagasawa, S. Ohya, K. Sakamoto, and M. Sakamoto, “Gauge-Fixing and Residual Symmetries in Gauge/Gravity Theories with Extra Dimensions,” *Phys.Rev.* **D77** (2008) 065009, [arXiv:0801.0845 \[hep-th\]](#).
- [60] Y. Fujimoto, T. Nagasawa, S. Ohya, and M. Sakamoto, “Phase Structure of Gauge Theories on an Interval,” *Prog.Theor.Phys.* **126** (2011) 841–854, [arXiv:1108.1976 \[hep-th\]](#).
- [61] **Particle Data Group** Collaboration, J. Beringer *et al.*, “Review of Particle Physics (RPP),” *Phys.Rev.* **D86** (2012) 010001.
- [62] C. Csaki, C. Grojean, H. Murayama, L. Pilo, and J. Terning, “Gauge theories on an interval: Unitarity without a Higgs,” *Phys.Rev.* **D69** (2004) 055006, [arXiv:hep-ph/0305237 \[hep-ph\]](#).
- [63] N. Sakai and N. Uekusa, “Selecting gauge theories on an interval by 5D gauge transformations,” *Prog.Theor.Phys.* **118** (2007) 315–335, [arXiv:hep-th/0604121 \[hep-th\]](#).
- [64] K. Nishiwaki and K.-y. Oda, “Unitarity in Dirichlet Higgs Model,” *Eur.Phys.J.* **C71** (2011) 1786, [arXiv:1011.0405 \[hep-ph\]](#).
- [65] L. C. de Albuquerque and R. M. Cavalcanti, “Casimir effect for the scalar field under Robin boundary conditions: A Functional integral approach,” *J.Phys.* **A37** (2004) 7039–7050, [arXiv:hep-th/0311052 \[hep-th\]](#).
- [66] Z. Bajnok, L. Palla, and G. Takacs, “Casimir force between planes as a boundary finite size effect,” *Phys.Rev.* **D73** (2006) 065001, [arXiv:hep-th/0506089 \[hep-th\]](#).
- [67] M. Pawellek, “Quantum mass correction for the twisted kink,” *J.Math.Phys.* **42** (2009) 045404, [arXiv:0802.0710 \[hep-th\]](#).